Chiral Platinum Duphos Terminal Phosphido Complexes: Synthesis, Structure, Phosphido Transfer, and Ligand Behavior

Corina Scriban,[†] David S. Glueck,*[,†] Antonio G. DiPasquale,[‡] and Arnold L. Rheingold[‡]

6128 Burke Laboratory, Department of Chemistry, Dartmouth College, Hanover, New Hampshire 03755, and Department of Chemistry and Biochemistry, University of California, San Diego, 9500 Gilman Drive, La Jolla, California 92093

Received July 7, 2006

Treatment of Pt halide precursors with the secondary phosphine PHMe(Is) in the presence of the base $NaOSiMe_3$ gave the terminal phosphido complexes Pt(Duphos)(Ph)(PMeIs) (Is = 2,4,6-(i-Pr)$_3$C$_6$H$_2$, Duphos = (*R*,*R*)-Me-Duphos (**1**), (*R*,*R*)-*i*-Pr-Duphos (**2**)), Pt((*R*,*R*)-Me-Duphos)(X)(PMeIs) (X = I (**3**), Cl (**4**)), and Pt((*R*,*R*)-Me-Duphos)(PMeIs)$_2$ (**5**). Low-barrier pyramidal inversion in the phosphido complexes was investigated by ^{31}P NMR spectroscopy. Protonation of **1**−**5** with HBF_4 gave the secondary phosphine complexes [Pt(Duphos)(Ph)(PHMeIs)][BF_4] (Duphos = (*R*,*R*)-Me-Duphos (**6**), (*R*,*R*)-*i*-Pr-Duphos) (**7**)), [Pt((*R*,*R*)-Me-Duphos)(X)(PHMeIs)][BF_4] (X = I (**8**), Cl (**9**)), and [Pt((*R*,*R*)-Me-Duphos)(PHMeIs)$_2$][BF_4]$_2$ (**10**); cations **6**, **9**, and **10** were prepared independently from Pt chloride precursors using Ag(I) salts and PHMe(Is) and then deprotonated to yield phosphido complexes **1**−**5**. Oxidation of the phosphido ligands in **4** and **5** with H_2O_2 gave Pt((*R*,*R*)-Me-Duphos)(Cl)(P(O)MeIs) (**11**) and Pt((*R*,*R*)-Me-Duphos)(P(O)-MeIs)$_2$ (**12**), respectively. Complexes **1**−**6**, **9**, and **11** were structurally characterized by X-ray crystallography; structural and ^{31}P NMR results suggest the trans influence order P(O)MeIs > PMeIs > PHMe(Is). Reaction of **1** with [Pd(allyl)Cl]$_2$, followed by treatment with dppe, gave Pt((*R*,*R*)-Me-Duphos)-(Ph)(Cl), PMeIs(allyl) (**13**), and Pd(dppe)$_2$. Treatment of **1** with Pd(P(o-Tol)$_3$)$_2$ gave an equilibrium mixture containing the two-coordinate palladium complex Pd(P(o-Tol)$_3$)(μ-PMeIs)Pt((*R*,*R*)-Me-Duphos)(Ph) (**14**), Pd(P(o-Tol)$_3$)$_2$, P(o-Tol)$_3$, and **1**.

Introduction

Terminal metal phosphido complexes (M−PR_2) contain nucleophilic phosphorus centers which can act as ligands to other metals; these "metallophosphines" form the bimetallic complexes M−PR_2−M′. The metal substituent M may result in cooperative reactivity[1] or simply modify the properties of the phosphine.[2] For example, chiral-at-Re complexes such as Re(η^5-$C_5H_4PPh_2$)(PPh_3)(NO)(PPh_2) have been used in asymmetric catalysis.[3] Another class of chiral metallophosphines is phosphorus-stereogenic, as in **A** and **B** (Scheme 1),[4] which contain an additional chiral group (the diphosphine in **A** and the Ta in **B)**. Because of the low barrier to pyramidal inversion at P in metallophosphines,[5] these compounds are expected to exist as mixtures of rapidly interconverting diastereomers. Thus, the Fe−phosphido complex **A** was a 4:1 mixture of diastereomers at −65 °C, but only one diastereomer of **B** was observed by NMR spectroscopy.[4]

Scheme 1. Diastereoselective Complexation by P-Stereogenic Metallophosphines[a]

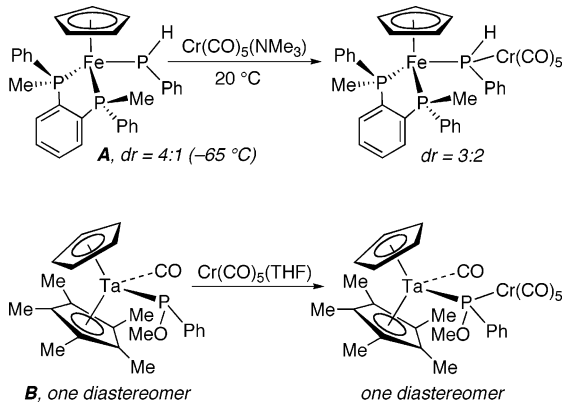

[a] dr = diastereomer ratio.

A thermodynamic preference for one diastereomer (as seen for **B**) and/or a kinetic difference in the rates of complexation of such ligands to a second metal might result in "self-resolving" P-stereogenic metallophosphines and their metal complexes, which could be useful in asymmetric catalysis. For example, reaction of **B** with $Cr(CO)_5$(THF) gave a single diastereomer of the Ta−Cr product (without, however, absolute stereocontrol at Ta or P). A similar reaction of **A** gave a 3:2 mixture of diastereomers, which were separated by crystallization.[4]

To investigate the rational design and application of such P-stereogenic metallophosphines, we report here the preparation, structure, and reactivity of a class of chiral Pt(Duphos) terminal phosphido complexes (Chart 1). As in the Fe complex **A**, a chiral diphosphine was intended to provide thermodynamic control

* To whom correspondence should be addressed. E-mail: glueck@dartmouth.edu

[†] Dartmouth College.

[‡] University of California, San Diego.

(1) (a) Stephan, D. W. *Coord. Chem. Rev.* **1989**, *95*, 41−107. (b) Baker, R. T.; Fultz, W. C.; Marder, T. B.; Williams, I. D. *Organometallics* **1990**, *9*, 2357−2367.

(2) For a recent example, see: Giner Planas, J.; Gladysz, J. A. *Inorg. Chem.* **2002**, *41*, 6947−6949.

(3) (a) Delacroix, O.; Gladysz, J. A. *Chem. Commun.* **2003**, 665−675. (b) Zwick, B. D.; Arif, A. M.; Patton, A. T.; Gladysz, J. A. *Angew. Chem., Int. Ed.* **1987**, *26*, 910−912.

(4) For **A**, see: Hey, E.; Willis, A. C.; Wild, S. B. *Z. Naturforsch., B* **1989**, *44*, 1041−1046. For **B**, see: Challet, S.; Lavastre, O.; Moise, C.; Leblanc, J.-C.; Nuber, B. *New J. Chem.* **1994**, *18*, 1155−1161.

(5) Rogers, J. R.; Wagner, T. P. S.; Marynick, D. S. *Inorg. Chem.* **1994**, *33*, 3104−3110.

10.1021/om060614y CCC: $33.50
Publication on Web 09/19/2006

Chart 1. Pt(Duphos) Terminal Phosphido Complexes as P-Stereogenic Metallophosphines[a]

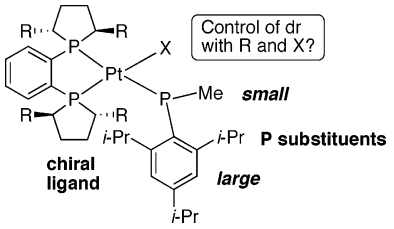

[a] X = Ph, R = Me (**1**), R = *i*-Pr (**2**); X = I (**3**), Cl (**4**), R = Me; X = PMe(Is), R = Me (**5**).

Scheme 2[a]

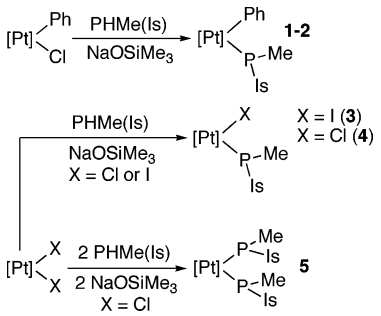

[a] [Pt] = Pt((*R*,*R*)-Me-Duphos) for **1** and **3**-**5**; [Pt] = Pt((*R*,*R*)-*i*-Pr-Duphos) for **2**.

of the phosphido stereocenter, via Duphos−phosphido interactions. However, to provide greater steric differentiation of the P substituents, the P−Ph group was replaced by the bulky aryl 2,4,6-(*i*-Pr)$_3$C$_6$H$_2$ (isityl = Is).[6] To investigate substituent effects on the diastereomer ratio (dr) in this class of metallophosphines, the chiral ancillary ligand and the Pt−X substituent were also varied.[7]

Results and Discussion

Synthesis and Structure of Pt(Duphos) Terminal Phosphido Complexes Treatment of Pt((*R*,*R*)-Me-Duphos)(Ph)(Cl)[8] or the *i*-Pr-Duphos analogue (see the Experimental Section) with the secondary phosphine PHMe(Is)[9] and the base NaOSiMe$_3$ gave the terminal phosphido complexes Pt(Duphos)(Ph)(PMeIs) (Duphos = (*R*,*R*)-Me-Duphos (**1**), (*R*,*R*)-*i*-Pr-Duphos (**2**)) in high yield. An analogous reaction of Pt((*R*,*R*)-Me-Duphos)I$_2$ gave the iodo phosphido complex Pt((*R*,*R*)-Me-Duphos)(I)(PMeIs) (**3**), even when an excess of PHMe(Is) and base was used (Scheme 2).[8]

Similarly, treatment of Pt((*R*,*R*)-Me-Duphos)Cl$_2$ with 1 or 2 equiv of the secondary phosphine and NaOSiMe$_3$ gave Pt((*R*,*R*)-Me-Duphos)(Cl)(PMeIs) (**4**) and Pt((*R*,*R*)-Me-Duphos)(PMeIs)$_2$ (**5**), respectively.[10] In contrast to the syntheses of **1**−**3**, however, it was difficult to control the stoichiometry of these reactions and obtain **4** free of **5**, or vice versa. Moreover, other phosphido complexes tentatively formulated as Pt((*R*,*R*)-Me-Duphos)(OSiMe$_3$)(PMeIs) and Pt((*R*,*R*)-Me-Duphos)(OH)(PMeIs), as well as other unidentified impurities, were formed; see the Experimental Section for details.

Scheme 3[a]

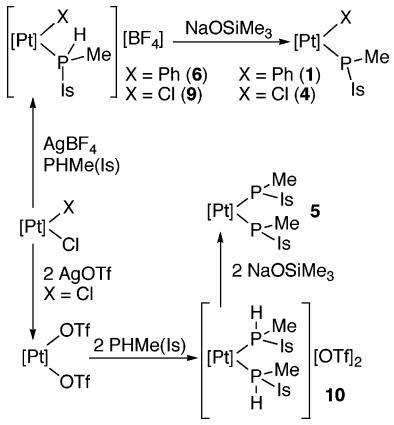

[a] [Pt] = Pt((*R*,*R*)-Me-Duphos).

Therefore, complexes **4** and **5** were also prepared by the multistep route shown in Scheme 3. Abstraction of chloride using Ag(I) salts, followed by treatment with PHMe(Is), gave the cationic secondary phosphine complexes **6**, **9**, and **10**, whose properties are described in more detail below. Deprotonation then gave phosphido complexes **1**, **4**, and **5**. Although this method also failed to provide pure **4** and **5**, they were characterized by spectroscopy and by X-ray crystallography (see below) and could be used to prepare derivatives.

The phosphido complexes **1**−**5** are yellow-to-orange crystalline solids. Their high air sensitivity made it very difficult to obtain satisfactory elemental analyses;[11] as described in the Experimental Section, analyses were often consistent with oxidation at the phosphido P. Indeed, deliberate oxidation of **4** and **5** gave Pt((*R*,*R*)-Me-Duphos)(Cl)(P(O)MeIs) (**11**) and Pt((*R*,*R*)-Me-Duphos)(P(O)MeIs)$_2$ (**12**), which are described below. However, protonation at P gave the cationic secondary phosphine complexes **6**−**10** (see Scheme 3 and below), which could be isolated in analytically pure form.[12]

Phosphido complexes **1**−**5** were characterized by multinuclear NMR spectroscopy; ^{31}P NMR data appear in Table 1. As previously observed for terminal Pt−phosphido complexes, the PMeIs group displayed characteristic trans J_{PP} and J_{Pt-P} values, which are smaller than those for tertiary phosphine ligands.[13] Because of peak overlap in the Duphos region, these species were most conveniently characterized by their PMeIs shifts. Low-temperature ^{31}P NMR spectroscopy showed the expected two diastereomers for **3** and **4** and three of the four diastereomers for **5**, but the results were more complicated for **1** and **2** (four diastereomers each). We believe the "extra" resonances within

(6) We showed earlier that Pd((*R*,*R*)-Me-Duphos)(Ph)(PMeIs) was a ca. 40:1 mixture of diastereomers at −60 °C (Moncarz, J. R.; Laritcheva, N. F.; Glueck, D. S. *J. Am. Chem. Soc.* **2002**, *124*, 13356−13357). These complexes decompose by P−C reductive elimination at room temperature, but the Pt analogues reported here are thermally stable.

(7) For the use of the phosphido complexes as catalyst precursors in asymmetric alkylation of PHMe(Is), see: (a) Scriban, C.; Glueck, D. S. *J. Am. Chem. Soc.* **2006**, *128*, 2788−2789. For the related use of chiral cationic Pt−bis(phosphine) moieties for the selective binding of chiral phosphines or amines, see: (b) Payne, N. C.; Stephan, D. W. *J. Organomet. Chem.* **1981**, *221*, 223−230. (c) Payne, N. C.; Stephan, D. W. *J. Organomet. Chem.* **1982**, *228*, 203-215.

(8) Brunker, T. J.; Blank, N. F.; Moncarz, J. R.; Scriban, C.; Anderson, B. J.; Glueck, D. S.; Zakharov, L. N.; Golen, J. A.; Sommer, R. D.; Incarvito, C. D.; Rheingold, A. L. *Organometallics* **2005**, *24*, 2730−2746.

(9) Brauer, D. J.; Bitterer, F.; Dorrenbach, F.; Hessler, G.; Stelzer, O.; Kruger, C.; Lutz, F. *Z. Naturforsch., B* **1996**, *51*, 1183−1196.

(10) Wicht, D. K.; Zhuravel, M. A.; Gregush, R. V.; Glueck, D. S.; Guzei, I. A.; Liable-Sands, L. M.; Rheingold, A. L. *Organometallics* **1998**, *17*, 1412−1419.

(11) This phenomenon has been observed for related electron-rich terminal phosphido complexes which could also not be isolated in analytically pure form; see: Giner Planas, J.; Hampel, F.; Gladysz, J. A. *Chem. Eur. J.* **2005**, *11*, 1402−1416.

(12) For protonation of air-sensitive tertiary phosphines to yield air-stable phosphonium salts, see: Netherton, M. R.; Fu, G. C. *Org. Lett.* **2001**, *3*, 4295−4298.

(13) Zhuravel, M. A.; Glueck, D. S.; Zakharov, L. N.; Rheingold, A. L. *Organometallics* **2002**, *21*, 3208−3214 and references therein.

Table 1. Low-Temperature $^{31}P\{^1H\}$ NMR Data for the Phosphido Complexes[a]

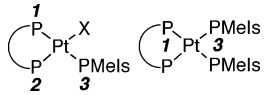

complex	T (°C)	$\delta(P_1)$ (J_{Pt-P})	$\delta(P_2)$ (J_{Pt-P})	$\delta(P_3)$ (J_{Pt-P})	J_{12}	J_{13}	J_{23}	dr[b]
Pt(Me-Duphos)(Ph)(PMeIs) (**1a**)[c]	−75	56.5 (1653)	57.3 (1868)	−55.9 (889)		136		98
1b				−47.3 (∼940)		136		2.2
1c				−49.5		142		1.2
1d				−51.6		134		1
Pt(*i*-Pr-Duphos)(Ph)(PMeIs) (**2a**)[c]	−60	54.6 (1683)	48.2 (1838)	−67.1 (903)	4	129	6	152
2b				−58.5 (875)		129		1
2c		56.1 (1704)	55.4 (1782)	−45.1 (951)		139		24
2d		55.1 (1668)	53.8 (1827)	−48.0 (877)		140		23
Pt(Me-Duphos)(I)(PMeIs) (**3a**)	−40	64.0 (1575)	54.1 (3954)	−69.6 (820)	21	113	17	8
3b		65.8 (1633)	65.0 (3876)	−42.5 (935)		110		1
Pt(Me-Duphos)(Cl)(PMeIs) (**4a**)	−20	69.3 (1607)	53.5 (4006)	−56.3 (804)	13	124	13	23
4b		72.2 (1668)	58.1 (3978)[d]	−37.2 (900)[d]		126	11	1
Pt(Me-Duphos)$(PMeIs)_2$ (**5a**)	−50	66.2 (1679)		−62.9 (887)	11	84		13
5b		52.1 (1859)		−48.3 (1001)	12	109	11	13
5c		60.6 (1597)		−64.5 (929)	13	98	7	1

[a] All Duphos ligands have the *R,R* configuration. Chemical shifts are given in ppm (85% H_3PO_4 external standard) and coupling constants in Hz. The solvent was THF-d_8. For atom labeling, see the figure above. In several cases (especially for minor diastereomers), it was not possible to assign Duphos P resonances; therefore, they are omitted. [b] dr = diastereomer ratio, from integration of the ^{31}P NMR spectra at −50 °C. [c] In addition to the expected diastereomers, which differ in configuration at P3, more diastereomers were observed for complexes **1** and **2**. The "extra" ones are assigned as rotamers (see the text for discussion). [d] Broad peaks.

each group of signals are due to conformational isomers, perhaps resulting from slow rotation about the P−C(Is) bond, as observed in low-temperature spectra of the analogous complexes Pt(dppe)$(C(O)C_3F_7)$(PPhAr) (Ar = *o*-$MeOC_6H_4$, Is, Mes, Mes-F_9; Mes = 2,4,6-$Me_3C_6H_2$; Mes-F_9 = 2,4,6-$(CF_3)_3C_6H_2$).[14]

The effect of substituents on the thermodynamics of the diastereomers with different configurations at the phosphido stereocenter was assessed by measuring diastereomer ratios of **1**−**5** at −50 °C (Table 1). The Me-Duphos complex **1** was a 98:1:1.2:2.2 mixture of isomers, which displayed similar PMeIs ^{31}P NMR chemical shifts. Assuming that the three minor isomers all have the same configuration at P means this is a 22:1 ratio of diastereomers whose main difference is the P stereochemistry, while the ratio might be larger if one or more of the minor peaks are due to a rotamer of the major diastereomer. For the *i*-Pr-Duphos complex **2**, a 152:1:24:23 mixture was observed. In this case, the two groups of distinctly different PMeIs chemical shifts suggest that the major diastereomer is a 152:1 mixture of rotamers, while the minor diastereomer is a ∼1:1 mixture of rotamers. With this assumption, the ratio of "invertomers" is about 3:1. Thus, the more sterically demanding *i*-Pr-Duphos ligand provided reduced stereocontrol.

Similarly, comparison of diastereomer ratios for the Me-Duphos complexes **3** and **4** showed that the smaller chloro group (23:1) gave a higher dr value than did an iodo ligand (8:1). Finally, three of the potential four diastereomers of the bis(phosphido) complex **5** were observed; two were thermodynamically preferred at low temperature (ca. 13:13:1). As expected, the diastereomer preference in complexes **1**−**5** was more pronounced than in the related Pt((*R,R*)-Me-Duphos)(Me)(PPh(*i*-Bu)), which contains P substituents of similar size (dr = 1.4:1, −40 °C, toluene-d_8).[15c]

Coalescence behavior involving both types of diastereomers was observed by variable-temperature ^{31}P NMR spectroscopy (Table 2). The spectra of halide complexes **3** and **4** were the simplest, since only two diastereomers were observed at low temperature; their signals coalesced on warming. Measurement of the coalescence temperatures for the three different P nuclei provided approximate free energies of activation for the dynamic process,[16] which is presumably a composite of P inversion and rotation about the Pt−P bond.[14] Analysis of the coalescence behavior of the two major sets of signals for the bis(phosphido) complex **5** yielded a barrier similar in magnitude, but we cannot tell if this involves one or two P inversions, since the absolute configuration at the phosphido stereocenters is not known. For the *i*-Pr-Duphos complex **2**, coalescence of the signals due to the "invertomers" occurred before that of the rotamers; thus, it was possible to obtain approximate barriers to both processes, which are similar in magnitude. The low intensities of the peaks due to the minor diastereomers of **1** prevented similar measurements in this case.

As in related Pt−phosphido complexes, the inversion/rotation barriers for **2**−**5** were low, about 10−12 kcal/mol (Table 2).[13−15] A similar barrier was observed for Pt((*R,R*)-Me-Duphos)(Me)(PPh(*i*-Bu)),[15c] which suggests that the bulky isityl group did not have a large effect.

The phosphido complexes **1**−**5** were also characterized by X-ray crystallography (Figures 1−5, Tables 3 and 4, and Supporting Information). Although two (or more) diastereomers of each complex were observed by NMR spectroscopy in solution, only one was observed in these single-crystal structures. Moreover, the (R_P)-PMeIs absolute configuration was observed in complexes **1**, **3**, and **4** and for both phosphido groups of **5**. The latter observation means that **5** has approximate C_2 symmetry (Figure S1, Supporting Information). The (S_P)-PMeIs group in **2** is consistent with this trend, since, despite their identical *R,R* labels, (*R,R*)-Me-Duphos and (*R,R*)-*i*-Pr-Duphos have opposite absolute configurations because of the priority sequence rule definitions.[17] These observations could be explained if this class of (*R,R*)-Me-Duphos/(R_P)-PMeIs or (*R,R*)-*i*-Pr-Duphos/(S_P)-PMeIs diastereomers were

(14) Wicht, D. K.; Glueck, D. S.; Liable-Sands, L. M.; Rheingold, A. L. *Organometallics* **1999**, *18*, 5130−5140.

(15) (a) Wicht, D. K.; Kovacik, I.; Glueck, D. S.; Liable-Sands, L. M.; Incarvito, C. D.; Rheingold, A. L. *Organometallics* **1999**, *18*, 5141−5151. (b) Kovacik, I.; Wicht, D. K.; Grewal, N. S.; Glueck, D. S.; Incarvito, C. D.; Guzei, I. A.; Rheingold, A. L. *Organometallics* **2000**, *19*, 950−953. (c) Scriban, C.; Wicht, D. K.; Glueck, D. S.; Zakharov, L. N.; Golen, J. A.; Rheingold, A. L. *Organometallics* **2006**, *25*, 3370−3378.

(16) Friebolin, H. In *Basic One- and Two-Dimensional NMR Spectroscopy*, 2nd ed.; VCH: New York, 1993; pp 287−314.

(17) Burk, M. J.; Feaster, J. E.; Nugent, W. A.; Harlow, R. L. *J. Am. Chem. Soc.* **1993**, *115*, 10125−10138.

Table 2. Variable-Temperature ^{31}P NMR Data (THF-d_8) for Pt(Duphos) Phosphido Complexes[a]

complex	resonance[b]	δ (ppm)	$\Delta\nu$ (Hz)	T_c (K)	$\Delta G_c^{\ddagger}$ (kcal/mol)
Pt(*i*-Pr-Duphos)(Ph)(PMeIs) (**2a**,**b**/**2c**,**d**)[c]	P1	55.2, 54.1	223	263	12.1
	P3	−42.9, −65.3	4452	288	11.6
Pt(*i*-Pr-Duphos)(Ph)(PMeIs) (**2c**,**d**)[d]	P1	56.1, 55.1	202	243	11.2
	P2	55.4, 53.8	324	243	11.0
	P3	−45.1, −48.0	587	243	10.7
Pt(Me-Duphos)(I)(PMeIs) (**3**)	P1	64.0, 65.8	364	263	11.8
	P2	54.1, 65.0	2206	243	10.0
	P3	−69.6, −42.5	5484	283	11.3
Pt(Me-Duphos)(Cl)(PMeIs) (**4**)	P1	69.3, 72.2	587	283	12.5
	P2	53.5, 58.1	931	283	12.3
Pt(Me-Duphos)(PMeIs)$_2$ (**5**)	P1/P2	66.2, 52.1	2853	288	11.8
	P3/P4	−48.3, −62.9	2914	288	11.8
Pt(Me-Duphos)(Me)(PPh(*i*-Bu))[e]	P1	69.6, 67.8	809	283	12.8
	P3	−57.3, −63.9	1350	313	13.4

[a] All Duphos ligands have the *R,R* configuration. The solvent was THF-d_8. Chemical shifts and $\Delta\nu$ values are taken from slow-exchange spectra at −20 °C for invertomers **2a**,**b**/**2c**,**d**, −60 °C for rotamers **2c**/**2d**, −40 °C for **3**, −20 °C for **4**, and −40 °C for **5**. Estimated errors are different for each resonance; "typical" errors are 5 Hz in $\Delta\nu$, 10 °C in T_c, and 0.5 kcal/mol in $\Delta G_c^{\ddagger}$. [b] See Table 1 for the P labeling scheme. [c] Interconversion of "invertomers", which are assumed, on the basis of the large difference in P3 chemical shifts, to have different configurations at the phosphido P. [d] Interconversion between rotamers, which are assumed to have the same configurations at the phosphido P. [e] Reference 15c.

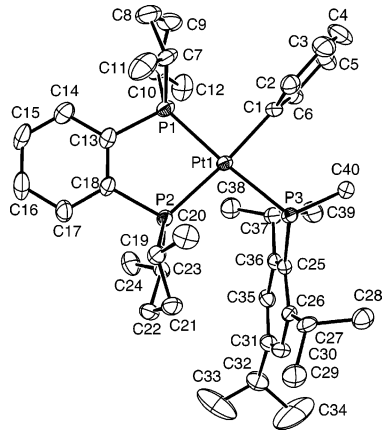

Figure 1. ORTEP diagram of Pt((*R,R*)-Me-Duphos)(Ph)(PMeIs) (**1**).

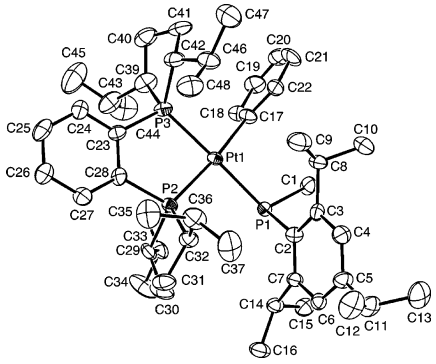

Figure 2. ORTEP diagram of one of the two independent molecules of Pt((*R,R*)-*i*-Pr-Duphos)(Ph)(PMeIs) (**2**).

favored in the crystallization process and/or if the crystals chosen for structure determination were not representative of the bulk sample.

Although *i*-Pr-Duphos is significantly more bulky than Me-Duphos, only small differences were observed in the structures of **1** and **2**. Varying the other ancillary ligand (the Pt−X group) led to larger structural changes. The Pt−PMeIs bond lengthened from 2.3761(13) Å in the Pt−Ph complex **1** to 2.3926(16) Å in the chloro complex **4**, 2.3996(19) Å in the iodo complex **3**, and 2.4117(10) and 2.3859(10) Å in the bis(phosphido) complex **5**, consistent with greater steric crowding in these cases. Although direct comparison to the Pt−phosphido bond lengths in Pt((*R,R*)-Me-Duphos)(H)(PPhIs) (**C**)[15b] and Pt((*R,R*)-Me-Duphos)(Me)-(PPh(*i*-Bu)) (**D**)[15c] is difficult, since the Pt−X group was also varied, those in **1**−**5** are similar, suggesting that the bulky isityl (Is) group does not constrain the Pt−phosphido bond length. Indeed, the shortest Pt−PR$_2$ bond in the series was observed for **C**, with the bulkiest phosphido ligand, perhaps because of the small size of the hydride ligand.

Similarly, the Pt−P1 (trans to PMeIs) bond was slightly longer in **3** and **5** (2.2962(18) and 2.3063(10) Å, respectively) than in **1** (2.2849(14) Å), consistent with the steric effects described above; the iodo and phosphido ligands in **3** and **5** appear to be more sterically demanding than Cl in **4**, for which the Pt−P1 distance was 2.2851(15) Å. The Pt−P2 (trans to X)

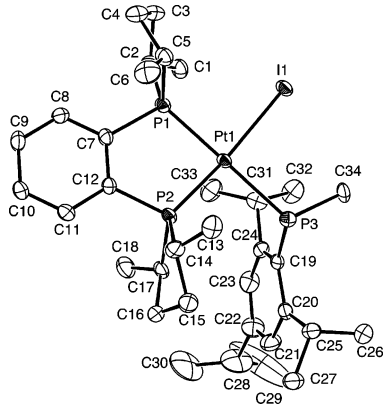

Figure 3. ORTEP diagram of one of the two independent molecules of Pt((*R,R*)-Me-Duphos)(I)(PMeIs) (**3**).

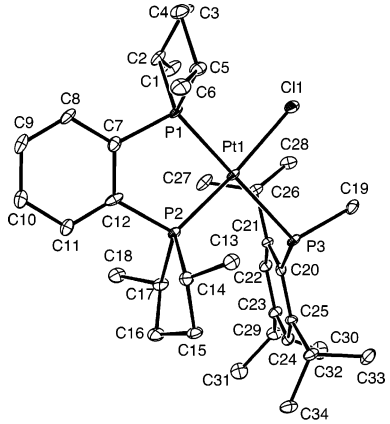

Figure 4. ORTEP diagram of Pt((*R,R*)-Me-Duphos)(Cl)(PMeIs)·C_6D_6 (**4**). Hydrogen atoms and the solvent molecule are omitted.

Table 3. Crystallographic Data for the Complexes Pt((*R*,*R*)-Me-Duphos)(X)(PMeIs) (X = Ph (1), Cl (3), I (4·C_6D_6), PMeIs (5)), Pt((*R*,*R*)-*i*-Pr-Duphos)(Ph)(PMeIs) (2), [Pt((*R*,*R*)-Me-Duphos)(X)(PHMeIs)][BF_4] (X = Ph (6·CH_2Cl_2), Cl (9·CH_2Cl_2)), and Pt((*R*,*R*)-Me-Duphos)(Cl)(P(O)MeIs) (11·0.5C_7H_8)[a]

	1	2	3	4·C_6D_6	5	6·CH_2Cl_2	9·CH_2Cl_2	11·0.5C_7H_8
formula	$C_{40}H_{59}P_3Pt$	$C_{48}H_{75}P_3Pt$	$C_{34}H_{54}IP_3Pt$	$C_{34}H_{54}ClP_3Pt$·C_6D_6	$C_{50}H_{80}P_4Pt$	$C_{40}H_{60}P_3Pt$-BF_4·CH_2Cl_2	$C_{34}H_{55}ClP_3Pt$-BF_4·CH_2Cl_2	$C_{75}H_{116}Cl_2O_2P_6Pt_2$
formula wt	827.87	939.58	877.67	870.33	1000.11	998.60	874.04	1696.58
space group	$P2_12_12_1$	$P2_1$	$P2_12_12_1$	$P2_12_12_1$	$P2_12_12_1$	$P2_12_12_1$	$P2_12_12_1$	$P2_1$
a, Å	10.3213(18)	12.5490(9)	10.2606(10)	9.935(2)	9.9966(15)	11.0214(18)	8.326(4)	10.049(2)
b, Å	15.712(3)	23.1943(16)	18.4791(19)	17.704(4)	19.761(2)	13.219(2)	20.847(10)	40.208(8)
c, Å	28.338(5)	18.1986(12)	41.283(4)	22.109(5)	24.836(4)	30.925(5)	23.51(11)	10.130(2)
α, deg	90	90	90	90	90	90	90	90
β, deg	90	96.7110(10)	90	90	90	90	90	107.384(3)
γ, deg	90	90	90	90	90	90	90	90
V, Å^3	4595.7(14)	5260.7(6)	7827.5(14)	3888.7(14)	4906.1(12)	4505.6(13)	4081(19)	3906.1(14)
Z	4	4	8	4	4	4	4	2
D(calcd), g/cm^3	1.197	1.186	1.490	1.486	1.354	1.472	1.561	1.442
μ(Mo Kα), mm^{-1}	3.179	2.785	4.516	3.827	3.022	3.383	3.795	3.810
temp, K	218(2)	213(2)	203(2)	100(2)	100(2)	218(2)	208(2)	208(2)
$R(F)$, %[b]	3.26	4.72	3.86	4.23	2.84	2.90	6.41	4.91
$R_w(F^2)$, %[b]	8.55	11.41	8.72	9.33	5.36	6.38	12.29	11.61

[a] A Bruker CCD diffractometer was used in all cases. [b] Quantity minimized: $R_w(F^2) = \sum[w(F_o^2 - F_c^2)^2]/\sum[(wF_o^2)^2]^{1/2}$; $R = \sum\Delta/\sum(F_o)$, $\Delta = |(F_o - F_c)|$; $w = 1/[\sigma^2(F_o^2) + (aP)^2 + bP]$, $P = [2F_c^2 + \mathrm{Max}(F_o^2,0)]/3$.

Table 4. Selected Bond Lengths and Angles for the Phosphido Complexes Pt((*R*,*R*)-Me-Duphos)(Ph)(PMeIs) (1), Pt((*R*,*R*)-*i*-Pr-Duphos)(Ph)(PMeIs) (2), Pt((*R*,*R*)-Me-Duphos)(I)(PMeIs) (3), Pt((*R*,*R*)-Me-Duphos)(Cl)(PMeIs)·C_6D_6 (4·C_6D_6), and Pt((*R*,*R*)-Me-Duphos)$(PMeIs)_2$ (5) and the Previously Reported Pt((*R*,*R*)-Me-Duphos)(H)(PPhIs) (C) and Pt((*R*,*R*)-Me-Duphos)(Me)(PPh(*i*-Bu)) (D)[a]

	1	2[b]	3[b]	4·C_6D_6	5[c]	C[d]	D[f]
Pt−P1	2.2849(14)	2.288(2)	2.2962(18)	2.2851(15)	2.3063(10)	2.226(4)	2.243(3)
Pt−P2	2.3028(13)	2.293(2)	2.2267(18)	2.2050(16)	2.3103(10)	2.298(5)	2.273(3)
Pt−P3	2.3761(13)	2.370(2)	2.3996(19)	2.3926(16)	2.4117(10)	2.335(5)	2.372(4)
Pt−X	2.070(5)	2.073(9)	2.6496(6)	2.3802(15)	2.3859(10)	ND[e]	2.13(3)[g]
P1−Pt−P2	85.66(5)	86.07(9)	86.35(6)	87.56(6)	84.98(4)	86.83(18)	86.44(12)
P1−Pt−P3	171.47(5)	175.60(9)	172.28(7)	173.38(6)	173.89(4)	169.72(18)	177.4(4)
P1−Pt−X	89.83(14)	89.7(3)	87.67(5)	86.45(5)	94.84(4)	ND[e]	91.6(7)[g]
P2−Pt−P3	97.37(5)	94.98(9)	93.36(6)	91.11(6)	89.18(3)	100.89(16)	90.45(12)
P2−Pt−X	173.81(15)	172.6(3)	171.60(4)	172.72(6)	176.83(3)	ND[e]	171.0(9)[g]
P3−Pt−X	86.51(14)	88.7(3)	92.44(5)	94.36(5)	91.09(3)	ND[e]	91.5(7)[g]
P3 angles	98.8(2)	98.2(4)	98.5(3)	97.4(3)	93.43(18)	102.2(5)	98.4(11)
	109.95(15)	111.4(4)	110.6(2)	106.1(2)	114.85(14)	112.5(4)	109.7(5)
	111.89(19)	113.7(3)	112.2(3)	113.03(19)	113.13(12)	111.9(4)	98.1(9)
∑P3 angles	320.6(2)	323.3(4)	321.3(3)	316.5(4)	321.41(18)	326.6(5)	306.2(11)

[a] Labeling of the phosphorus atoms is as in Table 1: P3 = phosphido, P1 = trans Duphos, P2 = cis Duphos. Note that the labeling shown in ORTEP diagrams of complexes **2** and **4** (Figures 2 and 4) is slightly different. In bis-phosphido complex **5**, X = PMe(Is), P4 is cis to P1 and trans to P2. [b] Two molecules in the unit cell; average bond lengths and angles are reported. [c] The "P3 angles" and "ΣP3 angles" entries for **5** are average values for the two phosphido ligands, P3 and P4. [d] See ref 15b. [e] The hydride ligand was not located in **C**, so associated bond lengths and angles were not determined (ND). [f] Reference 15c. [g] The Pt-Me group in **D** was disordered over two positions; average bond lengths and angles are reported.

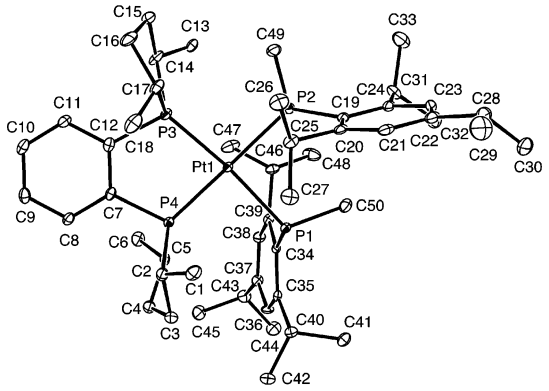

Figure 5. ORTEP diagram of Pt((*R*,*R*)-Me-Duphos)$(PMeIs)_2$ (**5**).

bonds reflected the trans influence, with those trans to Ph in **1** and **2** (2.3028(13) and 2.293(2) Å, respectively) and PMeIs in **5** (2.3063(10) and 2.3103(10) Å) longer than the ones trans to I in **3** (2.2267(18) Å) and to Cl in **4** (2.2050(16) Å). The internal comparison in **1** (and **2**) suggests that Ph has a larger trans influence than PMeIs, although the differences are small and ^{31}P NMR data indicate the opposite ordering (J_{Pt-P} trans to Ph > J_{Pt-P} trans to PMeIs; see Table 1).[18] The Pt−halide bonds in the iodo complex **3** (2.6496(6) Å) and chloro complex **4** (2.3802(15) Å) were essentially unchanged from those in Pt((*R*,*R*)-Me-Duphos)I_2 (2.6434(10) and 2.6151(11) Å)[8] and Pt((*R*,*R*)-Me-Duphos)Cl_2·CH_2Cl_2 (2.3828(12) and 2.3881(12) Å).[10]

Phosphido complexes **1**−**5** adopted approximate square-planar geometries, with minor distortions. The angles at the PMeIs group varied little in the series, with the sum ranging from 316.5(4) to 323.3(4)°. In comparison to idealized values of 328.5° for a tetrahedral geometry and 360° for trigonal-planar coordination, these observations are as expected for pyramidal phosphido ligands with a stereochemically active lone pair.[19] The smaller angle sum observed for the PPh(*i*-Bu) ligand in **D** suggests that steric effects are important in controlling the geometry at the phosphido P.

(18) Appleton, T. G.; Clark, H. C.; Manzer, L. E. *Coord. Chem. Rev.* **1973**, *10*, 335−422.

(19) Wicht, D. K.; Paisner, S. N.; Lew, B. M.; Glueck, D. S.; Yap, G. P. A.; Liable-Sands, L. M.; Rheingold, A. L.; Haar, C. M.; Nolan, S. P. *Organometallics* **1998**, *17*, 652−660.

Table 5. $^{31}P\{^{1}H\}$ NMR Data for the Cationic Secondary Phosphine Complexes 6−10 and Secondary Phosphido Oxide Complexes 11 and 12[a]

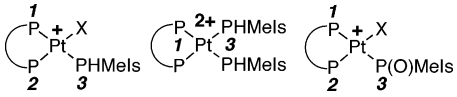

complex	$\delta(P_1)$ (J_{Pt-P})	$\delta(P_2)$ (J_{Pt-P})	$\delta(P_3)$ (J_{Pt-P})	J_{12}	J_{13}	J_{23}	dr[b]
[Pt(Me-Duphos)(Ph)(PHMeIs)][BF_4](**6a**)	63.1 (2623)	62.8 (1643)	−62.6 (2513)	8	372	18	14
6b	61.4 (2618)	67.6 (1691)	−55.2 (2472)	6	376	18	1
[Pt(*i*-Pr-Duphos)(Ph)(PHMeIs)][BF_4] (**7a**)	58.4 (2681)	57.3 (1656)	−66.1 (2510)	6	372	17	1.3[b]
7b	57.1 (2687)	53.7 (1631)	−60.3 (2481)	5	377	17	1[b]
[Pt(Me-Duphos)(I)(PHMeIs)][BF_4] (**8a**)	74.8 (2321)	65.0 (3102)	−72.0 (2213)		374	18	3
8b	73.4 (2289)	72.0 (3175)	−65.8 (2164)		383	15	1
[Pt(Me-Duphos)(Cl)(PHMeIs)][BF_4] (**9a**)	78.9 (2380)	62.9 (3282)	−60.3 (2227)	3	377	18	1
9b	78.8 (2356)	65.4 (3312)	−53.5 (2230)	3	379	17	1.4
[Pt(Me-Duphos)(PHMeIs)$_2$][OTf]$_2$ (**10a**)[c]	69.9 (2188)		−71.6 (2200)		298[d]		3.8
10b	78.2 (2275)		−68.0 (2237)[e]		289	19	1
10c	68.1 (2158)		−70.9 (2160)[e]		296	24	1.1
Pt(Me-Duphos)(Cl)(P(O)MeIs) (**11a**)	64.9 (1452)	56.0 (3918)	64.7 (2796)	9	431	16	28
11b	65.7[f]	60.1 (3913)	60.8[f]	9	432	17	1
Pt(Me-Duphos)(P(O)MeIs)$_2$ (**12a**)[g]	60.6 (1656)		50.4 (2954)		365		1
12b	51.3 (1864)		48.1 (3185)		360		1

[a] All Duphos ligands have the *R,R* configuration. The solvent was CD_2Cl_2, and the temperature was 21 °C. Coupling constants are given in Hz, with 85% H_3PO_4 as the external chemical shift standard. Complexes **6**−**9** were mixtures of two diastereomers, while **10** was a mixture of three diastereomers; one gave a well-resolved AA′XX′ pattern, while PHMe(Is) signals for the others were broad. See the Experimental Section for details. [b] dr = diastereomer ratio, from ^{31}P NMR integration after recrystallization. The initial ratio for **7** was 1.3:1, but recrystallization gave pure **7a**. [c] Spectra and diastereomer ratio for the BF_4 salt were similar. [d] AA′XX′ pattern with $J_{AX} = 298$, $J_{AX'} = -24$, $J_{AA'} = 32$, $J_{XX'} = 0$. [e] Broad peaks. [f] Low concentration of the minor diastereomer **11b** precluded measurement of J_{Pt-P}. [g] The ^{31}P NMR resonances for **12** were complicated multiplets consistent with AA′XX′ patterns from which the large trans J_{PP} coupling could be extracted.

Scheme 4[a]

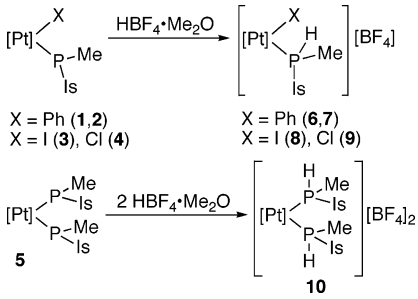

[a] [Pt] = Pt((*R,R*)-Me-Duphos), except for **2** and **7**, for which [Pt] = Pt((*R,R*)-*i*-Pr-Duphos).

Protonation and Oxidation of the Phosphido Complexes. Protonation of the phosphido complexes **1**−**4** with HBF_4 gave the secondary phosphine complexes **6**-**9** (Scheme 4), some of which were briefly mentioned above (Scheme 3). Initially, **6** and **7** were formed as 1:1 mixtures of diastereomers, but on standing in solution (for **6**) or recrystallization (**7**) one diastereomer was formed preferentially.[15a,20] Protonation of the bis(phosphido) complex **5** gave the bis(phosphine) dication **8** as a mixture of three of the expected four diastereomers.

Similarly, oxidation of **4** and **5** using H_2O_2 gave the phosphido oxide complexes **11** and **12**, in both cases as a mixture of two diastereomers (Scheme 5).[21] The diastereomer ratios of these products (11:1 and 1:1, respectively) were similar to those of the starting materials (Table 1), which might be explained if both phosphido diastereomers react at the same rate with H_2O_2. However, faster oxidation of the minor diastereomer of **4**, along with rapid diastereomer interconversion, could also result in a large product ratio.

Scheme 5[a]

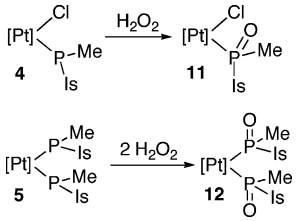

[a] [Pt] = Pt((*R,R*)-Me-Duphos).

As observed previously, protonation or oxidation resulted in increases in J_{PP} (trans) and J_{Pt-P}, consistent with increased s character in the Pt−P bond in the secondary phosphine and phosphido oxide complexes (see Table 5 for NMR data).[19] Note that, in one diastereomer of **11**, the ^{31}P NMR signals of the P(O)Me(Is) group and the Duphos P trans to it were accidentally coincident, and assignment was based on the relative J_{Pt-P} values for these signals.[22]

X-ray crystallographic studies on **6**, **9**, and **11** demonstrated the effects of protonation or oxidation of the phosphido complexes on their structures (Tables 3 and 6). A single crystal of **6**·CH_2Cl_2 had the R_P absolute configuration (Figure 6), as observed for the neutral precursor **1**, but the analogous chloro cation **9**·CH_2Cl_2 was S_P (Figure 7). Two molecules of **11**·$0.5C_7H_8$ were found in the unit cell; both had the R_P absolute configuration (Figure 8). Comparison of the structures in Figures 6 and 8 with those of their precursors in Figures 1 and 4 showed that, before and after quaternization at phosphorus, the conformations of the bulky groups were very similar. Although the S_P configuration in **9**·CH_2Cl_2 is unusual in this series, bond

(20) (a) Bader, A.; Nullmeyers, T.; Pabel, M.; Salem, G.; Willis, A. C.; Wild, S. B. *Inorg. Chem.* **1995**, *34*, 384−389. (b) References 7b,c.

(21) For other examples of oxidation of terminal phosphido complexes, see refs 11, 15c, and 22, as well as: Gallo, V.; Latronico, M.; Mastrorilli, P.; Nobile, C. F.; Suranna, G. P.; Ciccarella, G.; Englert, U. *Eur. J. Inorg. Chem.* **2005**, 4607−4616. Buhro, W. E.; Georgiou, S.; Hutchinson, J. P.; Gladysz, J. A. *J. Am. Chem. Soc.* **1985**, *107*, 3346−3348.

(22) On oxidation of *trans*-Pt(PCy_2H)$_2$(PCy_2)(Cl) to *trans*-Pt(PCy_2H)$_2$-(P(O)Cy_2)(Cl) (Mastrorilli, P.; Nobile, C. F.; Fanizzi, F. P.; Latronico, M.; Hu, C.; Englert, U. *Eur. J. Inorg. Chem.* **2002**, 1210−1218. Mastrorilli, P.; Latronico, M.; Nobile, C. F.; Suranna, G. P.; Fanizzi, F. P.; Englert, U.; Ciccarella, G. *Dalton Trans.* **2004**, 1117−1119), J_{Pt-P} for the phosphido ligand changed from 931 to 3078 Hz. Similarly, on oxidation of Pt(dppe)-(Me)(PPh(*i*-Bu)) to Pt(dppe)(Me)(P(O)Ph(*i*-Bu)), J_{Pt-P} for the phosphido ligand changed from 946 to 3006 Hz.[15c]

Table 6. Selected Bond Lengths and Angles for the Complexes Pt((*R*,*R*)-Me-Duphos)(Ph)(PMeIs) (1), Pt((*R*,*R*)-Me-Duphos)(Cl)(PMeIs)·C_6D_6 (4·C_6D_6), [Pt((*R*,*R*)-Me-Duphos)(Ph)(PHMeIs)][BF_4]·CH_2Cl_2 (6·CH_2Cl_2), [Pt((*R*,*R*)-Me-Duphos)(Cl)(PHMeIs)][BF_4]·CH_2Cl_2 (9·CH_2Cl_2), and Pt((*R*,*R*)-Me-Duphos)(Cl)(P(O)MeIs)·0.5C_7H_8 (11·0.5C_7H_8)[a]

	1	6·CH_2Cl_2	9·CH_2Cl_2	4·C_6D_6	11·0.5C_7H_8[c]
Pt−P1	2.2849(14)	2.2772(13)	2.279(3)	2.2851(15)	2.303(3)
Pt−P2	2.3028(13)	2.3096(11)	2.234(8)	2.2050(16)	2.221(3)
Pt−P3	2.3761(13)	2.3126(13)	2.347(3)	2.3926(16)	2.355(3)
Pt−X	2.070(5)	2.082(4)	2.356(7)	2.3802(15)	2.367(3)
P1−Pt−P2	85.66(5)	85.52(4)	86.58(11)	87.56(6)	86.31(10)
P1−Pt−P3	171.47(5)	177.11(4)	177.27(11)	173.38(6)	177.46(11)
P1−Pt−X	89.83(14)	90.21(13)	87.19(12)	86.45(5)	88.13(10)
P2−Pt−P3	97.37(5)	96.82(4)	95.74(12)	91.11(6)	92.79(10)
P2−Pt−X	173.81(15)	172.02(16)	170.97(10)	172.72(6)	171.67(12)
P3−Pt−X	86.51(14)	87.26(13)	90.34(12)	94.36(5)	92.51(10)
P3 angles	98.8(2)	103.9(13)[b]	107.7(6)[b]	97.4(3)	109.4(6) (av)[d]
	109.95(15)	120.38(15)	112.1(4)	106.1(2)	
	111.89(19)	118.19(19)	124.1(4)	113.03(19)	
∑P3 angles	320.6(2)	342.47(19)	343.9(6)	316.5(4)	*e*

[a] Labeling of the phosphorus atoms is as in Table 1: P3 = phosphido (secondary phosphine in **6** and **9**, phosphido oxide in **11**), P1 = trans Duphos, P2 = cis Duphos. Note that the labelings shown in the ORTEP diagrams of complexes **4** and **7** (Figures 4 and 7) are slightly different. [b] The P−H hydrogen atom was not located; therefore, the P3 angles involve only the Pt and C substituents. [c] Two independent molecules in the unit cell. Average bond lengths and angles are reported. [d] Average angle at P3 for the two independent molecules. [e] Complex **11** is unique in that bond angles involving all four P substituents could be measured (for the other complexes only three were available).

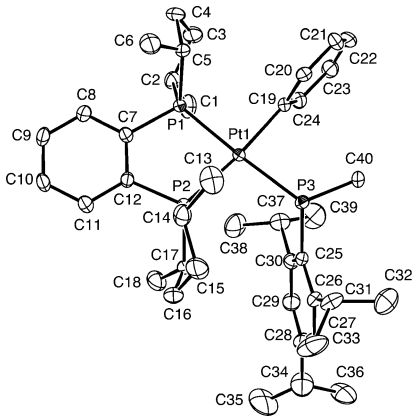

Figure 6. ORTEP diagram of [Pt((*R*,*R*)-Me-Duphos)(Ph)(PHMeIs)]-[BF_4]·CH_2Cl_2 (**6**·CH_2Cl_2). Hydrogen atoms, the BF_4 anion, and the solvent molecule are not shown.

lengths and angles in this structure showed no unusual features in comparison to the R_P analogues.

Protonation (**1** → **6**, **4** → **9**) resulted in significant structural changes (Table 6). Each of the P3 (phosphido/secondary phosphine) angles increased, consistent with the reduced steric demands of a proton in comparison to the P lone pair. The Pt−P3 (phosphido) bond shortened from 2.3761(13) to 2.3126(13) Å in **1**/**6** and from 2.3926(16) to 2.347(3) Å in **4**/**9**. These changes, which could be ascribed to removing repulsive Pt−P π interactions on protonation,[23] were also observed in the conversion of *trans,mer*-[$IrCl_2(PMe_2Ph)_3(PH_2)$] to *trans,mer*-[$IrCl_2(PMe_2Ph)_3(PH_3)$]$^+$,[24] but in the cyclometalated phosphido complex Pd(dppe)($CH_2C_6H_2Me_2P$(Mes)) (Mes = 2,4,6-$Me_3C_6H_2$),

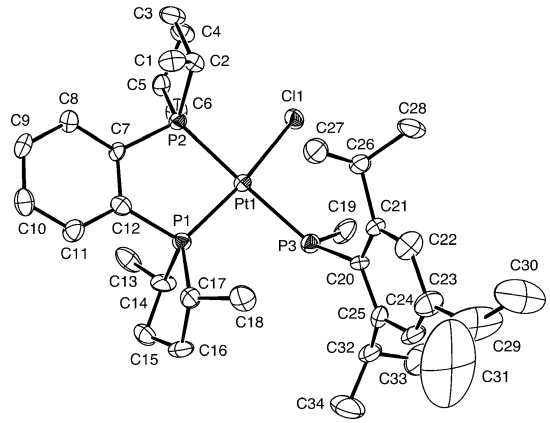

Figure 7. ORTEP diagram of [Pt((*R*,*R*)-Me-Duphos)(Cl)(PHMeIs)]-[BF_4]·CH_2Cl_2 (**9**·CH_2Cl_2). The anion and the disordered solvent molecule are not shown.

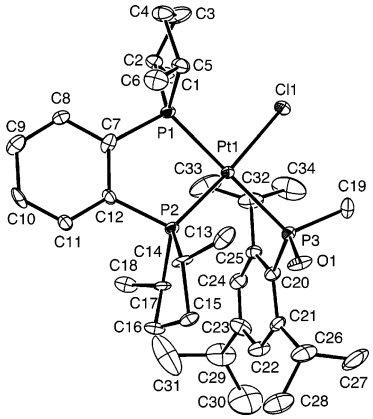

Figure 8. ORTEP diagram showing one of the two molecules of Pt((*R*,*R*)-Me-Duphos)(Cl)(P(O)MeIs)·0.5C_7H_8 (**11**·0.5C_7H_8) in the unit cell. Hydrogen atoms and the solvent molecule are omitted.

protonation led to a *longer* Pd−P bond.[13] Perhaps the constraints of the chelate ring in this case controlled the structural changes.

On protonation of **1**, the Pt−Ph and Pt−P2 (trans to Ph) bonds became slightly longer, changing from 2.070(5) to 2.082(4) Å and from 2.3028(13) to 2.3096(11) Å, respectively. The Pt−P2 (trans to Cl) bond in **9** also became longer (from 2.2050(16) to 2.234(8) Å), but the Pt−Cl bond contracted on protonation (from 2.3802(15) to 2.356(7) Å), perhaps as a result of increased Pt−Cl Coulombic attraction in the cation. The Pt−P1 (trans to PMeIs/PHMeIs) bonds in both pairs shortened from 2.2849(14) to 2.2772(13) Å in **1**/**6** and from 2.2851(15) to 2.279(3) Å in **4**/**9**, which suggests that the phosphido group has a larger trans influence than the secondary phosphine. This is consistent with the NMR data; J_{Pt-P} values for the Duphos P trans to PMeIs and PHMeIs in **1**/**6** were 1869 Hz (C_6D_6, room temperature) and 2620 Hz (CD_2Cl_2, average for the two diastereomers), respectively, while the values for **4**/**9** were 1637 Hz (THF-d_8, −20 °C, average for the two diastereomers) and 2368 Hz (CD_2Cl_2, average for the two diastereomers).[18] However, an opposite structural result was observed for both the Pd and the Ir complexes cited above. Reaching general conclusions on the structural effects of phosphido protonation, therefore, will require crystallographic studies of more such pairs of complexes.

Similarly, comparison of the structure of the phosphido complex **4** with that of its oxide **11** revealed effects similar to

(23) (a) Caulton, K. G. *New J. Chem.* **1994**, *18*, 25−41. (b) Holland, P. L.; Andersen, R. A.; Bergman, R. G. *Comments Inorg. Chem.* **1999**, *21*, 115−129.

(24) Deeming, A. J.; Doherty, S.; Marshall, J. E.; Powell, J. L.; Senior, A. M. *J. Chem. Soc., Dalton Trans.* **1993**, 1093−1100.

Scheme 6[a]

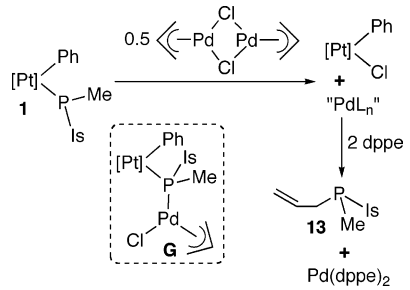

[a] [Pt] = Pt((*R*,*R*)-Me-Duphos), L = PMeIs(allyl).

those of protonation. On oxidation, the Pt−P3 bond shortened from 2.3926(16) to 2.355(3) Å, consistent as in the protonation case with erasing the repulsive Pt−P lone pair interaction. The phosphido P went from pyramidal (angle sum 316.5(4)°; compare 328.5° for the ideal tetrahedral geometry) to tetrahedral (average P angle 109.4(6)°), also consistent with removing the stereochemically active lone pair. The Pt−P2 bond lengthened slightly (from 2.2050(16) to 2.221(3) Å), while the Pt−Cl bond became shorter (2.3802(15) vs 2.367(3) Å), as observed for protonation (**4** and **9**). The Pt−P1 distance (trans to PMeIs/P(O)MeIs) changed from 2.2851(15) to 2.303(3) Å, suggesting a greater trans influence for the phosphido oxide ligand. This is consistent with the ^{31}P NMR data; J_{Pt-P} for the trans Duphos P changed from 1637 Hz (average for the two diastereomers) to 1452 Hz (major diastereomer; J_{Pt-P} was not observed for the minor one) on oxidation. The resulting trans influence order, from crystallographic and NMR data on chloro complexes **4**, **9**, and **11**, is then P(O)MeIs > PMeIs > PHMe(Is).

^{31}P NMR data on the bis(phosphido) complex **5** (Table 5) and its doubly protonated and oxidized derivatives **10** and **12** provided a similar ordering. Here, as in **4** and **11**, the average J_{Pt-P} for the trans Duphos P changed little on oxidation (from 1766 to 1760 Hz) but increased significantly on protonation (to 2207 Hz).

Pt(Duphos) Phosphido Complexes as Metalloligands. Since one diastereomer of **1** was thermodynamically favored, as desired (Chart 1), we briefly explored its metalloligand properties. Instead of complexation of the $Cr(CO)_5$ group (see Scheme 1), however, Pd moieties with potential use in catalysis were targeted.

Reaction with $[Pd(allyl)Cl]_2$ gave Pt((*R*,*R*)-Me-Duphos)(Ph)(Cl) as the major Pt(Duphos)-containing product (Scheme 6). A mixture of complexes we presume to be the zerovalent Pd[(PMeIs(allyl))]$_n$ was also observed by ^{31}P NMR spectroscopy. On treatment with excess dppe, these compounds disappeared, and $Pd(dppe)_2$ and the new phosphine PMeIs(allyl) (**11**) were formed.[25] After chromatographic separation, phosphine **13** was isolated in 71% yield (94% purity, 51% ee) and identified by NMR and high-resolution mass spectroscopy.[26] This reaction might occur by P−C reductive elimination from intermediate **G**[6] or by direct nucleophilic attack on the Pd−allyl group.[27]

Another approach to bimetallic phosphido-bridged Pt−Pd complexes was more successful. Treatment of **1** with Pd(P(*o*-Tol)$_3$)$_2$ gave an apparent equilibrium mixture containing **1**, Pd(P(*o*-Tol)$_3$)$_2$, the two-coordinate palladium complex Pd(P(*o*-Tol)$_3$)(μ-PMeIs)Pt((*R*,*R*)-Me-Duphos)(Ph) (**14**), and P(*o*-Tol)$_3$ (Scheme 7).[28] Formation of the products **14** and P(*o*-Tol)$_3$ was clearly favored, but the low solubility of Pd(P(*o*-Tol)$_3$)$_2$ prevented us from measuring K_{eq}. Additional **1** did not displace P(*o*-Tol)$_3$ from **14** at room temperature, and no exchange between **14** and P(*o*-Tol)$_3$ was observed on the NMR time scale. Attempts to isolate **14** were unsuccessful, but it could be characterized in the mixture as a 1:1 mixture of diastereomers by ^{31}P NMR spectroscopy. These diastereomers might differ in the absolute configuration at the μ-PMeIs group or result from slow rotation on the NMR time scale about the M−P bonds.

Scheme 7[a]

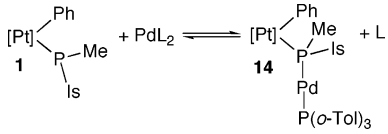

[a] [Pt] = Pt((*R*,*R*)-Me-Duphos), L = P(*o*-Tol)$_3$.

Quaternization of the phosphido group led to increased $J_{PP(trans)}$ (from 133 to 246 Hz (average)) and J_{Pt-P} (from 899 to 1550 Hz (average)) couplings in the Pt(Me-Duphos)(PMeIs) group, as observed for protonation and oxidation (see Table 5). Similarly, J_{Pt-P} for the Duphos P trans to PMeIs increased from 1621 to 1842 Hz (average), consistent with a decreased trans influence for the bridging phosphido ligand.

Conclusions

We prepared a series of Pt(Duphos) terminal phosphido complexes (**1**−**5**). The phosphido ligand, with a small methyl and a large isityl group, was intended to result in steric differentiation between the diastereomers of these complexes, causing a thermodynamic preference for one of them. As desired, this was observed, and the expected low barriers to inversion in the phosphido complexes were quantified by NMR spectroscopy. Despite the thermodynamic preference for one diastereomer of **1** and **2**, protonation gave kinetic mixtures of the secondary phosphine cationic complexes **6** and **7**, suggesting that the minor diastereomer reacted more quickly than the major one. Two of the four diastereomers of the bis(phosphido) complex **5** were favored, with similar results for the protonated dication **10** and the oxidized derivative **12**.

Complex **1**, with a large thermodynamic preference for one diastereomer, was designed to serve as a "self-resolving" metallophosphine. However, an attempt to complex it to the Pd(allyl) fragment resulted in phosphido transfer from Pt to the allyl group. More successful was the reaction of **1** with PdL_2 (L = P(*o*-Tol)$_3$). In this case, however, a ca. 1:1 mixture of diastereomeric Pt−Pd complexes **12** was formed in an apparent equilibrium. This points to a weakness in the original plan. It is not enough to design a P-stereogenic metallophosphine which exists primarily as a single diastereomer; it must also retain this P-based chirality on complexation. Moreover, the large size of metalloligand **1**, required for thermodynamic diastereoselection, presumably destabilized **14** sterically, contributing to its formation in an equilibrium. We are continuing studies of such metalloligands with these ideas in mind, in hopes of realizing highly selective, irreversible binding.

(25) Rosevear, D. T.; Stone, F. G. A. *J. Chem. Soc. A* **1968**, 164−167.

(26) The ^{1}H and ^{13}C NMR spectra of PMe(Is)(allyl), in comparison to those for PMe_2(allyl) (see Bampos, N.; Field, L. D.; Messerle, B. A.; Smernik, R. J. *Inorg. Chem.* **1993**, *32*, 4084−4088), were consistent with this formulation.

(27) The analogous reaction of Ru(Cp)(PEt_3)$_2$(PPh_2) with [Pd(allyl)(NCPh)$_2$][BF_4] gave a mixture of the cations [Cp(PEt_3)$_2$Ru(μ-PPh_2)Pd(NCPh)(allyl)]$^+$ and the allylphosphine complex [Ru(Cp)(PEt_3)$_2$(PPh_2(allyl))]$^+$.[11]

(28) Paul, F.; Patt, J.; Hartwig, J. F. *Organometallics* **1995**, *14*, 3030−3039. For use of Pd(P(*o*-Tol)$_3$)$_2$ in the synthesis of other PdL_2 complexes, see: Mann, G.; Shelby, Q.; Roy, A. H.; Hartwig, J. F. *Organometallics* **2003**, *22*, 2775−2789.

Experimental Section

All reactions and manipulations were performed in dry glassware under a nitrogen atmosphere at 20 °C in a drybox or using standard Schlenk techniques. Petroleum ether (bp 38−53 °C), ether, THF, toluene, and CH_2Cl_2 were dried using columns of activated alumina.[29] NMR spectra were recorded using Varian 300 and 500 MHz spectrometers. ^1H and ^{13}C NMR chemical shifts are reported vs Me_4Si and were determined by reference to the residual ^1H and ^{13}C solvent peaks. ^{31}P NMR chemical shifts are reported vs H_3PO_4 (85%) used as an external reference. Coupling constants are reported in Hz, as absolute values unless noted otherwise. Unless indicated, peaks in NMR spectra are singlets. Elemental analyses were provided by Schwarzkopf Microanalytical Laboratory or Quantitative Technology Inc. Mass spectra were recorded at the University of Illinois Urbana-Champaign.

Unless otherwise noted, reagents were from commercial suppliers. The following compounds were made according to literature methods: Pt(COD)(Ph)Cl) (COD = cyclooctadiene),[30] Pt((*R*,*R*)-Me-Duphos)Cl_2,[10] Pt((*R*,*R*)-Me-Duphos)I_2 and Pt((*R*,*R*)-Me-Duphos)(Ph)(Cl),[8] (*S*)-{Pd[$NMe_2CH(Me)C_6H_4$](Cl)}$_2$,[31] PHMe(Is),[9] and Pd(P(*o*-Tol)$_3$)$_2$.[28]

Pt((*R*,*R*)-Me-Duphos)(Ph)(PMeIs) (1). PHMe(Is) (141 mg, 0.56 mmol) was added with a microsyringe to a stirred slurry of Pt((*R*,*R*)-Me-Duphos)(Ph)(Cl) (346 mg, 0.56 mmol) in toluene (10 mL). $NaOSiMe_3$ (63.3 mg, 0.56 mmol) in toluene (10 mL) was added to the reaction mixture. As soon as Pt((*R*,*R*)-Me-Duphos)(Ph)(Cl) reacted, the mixture turned yellow; it was stirred for ∼3 h. The slurry was filtered through Celite, and the yellow filtrate was concentrated under vacuum. Petroleum ether was added to the yellow residue, yielding yellow crystals, which were washed further with petroleum ether and dried under vacuum, giving 415.5 mg (89%) of yellow crystals suitable for X-ray crystallography.

Anal. Calcd for $C_{40}H_{59}P_3Pt$: C, 58.03; H, 7.18. Found: C, 56.29; H, 7.41. Elemental analyses for carbon were consistently low, perhaps due to decomposition of the air-sensitive complex. Anal. Calcd for $C_{40}H_{59}P_3PtO$: C, 56.93; H, 7.05. We previously observed that the analogous Pt(Duphos) phosphido complex Pt((*R*,*R*)-Me-Duphos)(H)(PPhIs) also failed to give satisfactory analyses.[15b] Since we could not obtain good analyses on this or the other Pt−phosphido complexes, we protonated them with HBF_4 and isolated the resulting secondary phosphine complexes in analytically pure form after recrystallization (see below and refs 11 and 12). HRMS (*m*/*z*): calcd for $C_{40}H_{60}P_3Pt$ (MH^+), 828.3569; found, 828.3571. Complex **1** could also be prepared by deprotonation of the cation [Pt((*R*,*R*)-Me-Duphos)(Ph)(PHMe(Is))][OTf] (**6**; see below) with $NaN(SiMe_3)_2$ or other bases.

^1H NMR (C_6D_6): δ 8.07 (t, J = 6, J_{Pt-H} = 51, 1H, Ph ortho), 7.68 (t, J = 7, J_{Pt-H} = 51, 1H, Ph ortho), 7.37 (t, J = 7, 1H, Ar), 7.29 (t, J = 7, 1H, Ar), 7.21−7.18 (t, J = 6, 1H, Ar), 7.16 (2H, Is), 7.13−7.11 (m, 1H, Ar), 7.04 (t, J = 7, 1H, Ar), 6.97−6.90 (m, 2H, Ar), 5.16 (broad, 2H, CH, Is), 3.01−2.94 (m, 1H, CH), 2.89−2.81 (m, 1H, CH), 2.36−2.28 (m, 1H, CH), 2.17−2.08 (m, 1H, CH), 1.81−1.67 (m, 3H), 1.62 (dd, J = 17, 6, 6H, Me), 1.51 (d, J = 7, 6H, Me), 1.48−1.43 (m, 3H, P−Me), 1.40 (dd, J = 18, 7, 6H, Me), 1.28 (d, J = 8, 3H, Me), 1.27 (d, J = 7, 3H, Me), 0.99 (qd, J = 13, 5, 1H), 0.90−0.80 (m, 1H), 0.64 (dd, J = 14, 7, J_{Pt-H} = 53, 3H, Me), 0.58 (dd, J = 15, 8, 3H, Me). $^{13}C\{^1H\}$ NMR (C_6D_6): δ 154.7 (quat, Ar), 147.7 (quat, Ar), 147.2 (quat, Ar), 143.9−143.5 (m, Ar), 139.9 (Ph ortho), 137.6 (broad, Ph ortho), 133.1 (dd, J = 86, 14, Duphos), 130.0 (d, J = 78, Duphos), 128.2−127.7 (m, Ar overlapping with C_6D_6 signals), 122.2 (Ph para), 120.5 (broad, 2C, Is meta), 44.1 (d, J = 30, CH Duphos), 41.9−41.4 (m, CH Duphos), 37.8 (CH_2), 36.3 (CH_2), 35.5 (overlapping CH_2 and CH, Is), 34.7 (CH, Is), 34.3 (CH, Is), 32.8−32.1 (overlapping m and d, J = 42, 2CH Duphos), 27.2 (broad, CH_3, Is), 24.5 (CH_3, Is), 22.6 (CH_3, Is), 18.1 (dd, J = 20, 9, CH_3, Duphos), 15.6 (d, J = 9, CH_3, Duphos), 14.8 (d, J = 3, CH_3, Duphos), 14.5 (d, J = 2, CH_3, Duphos), 12.5−12.0 (m, P−CH_3). $^{31}P\{^1H\}$ NMR (C_6D_6): δ 58.3 (broad, J_{Pt-P} = 1869), 57.6 (dd, J = 133, 8, J_{Pt-P} = 1621), −51.8 (broad d, J = 133, J_{Pt-P} = 899). See Table 1 for low-temperature ^{31}P NMR data (four diastereomers).

Pt((*R*,*R*)-*i*-Pr-Duphos)(Ph)(Cl). A solution of (*R*,*R*)-*i*-Pr-Duphos (293 mg, 0.7 mmol) in CH_2Cl_2 (2 mL) was added dropwise to a solution of Pt(COD)(Ph)(Cl) (291 mg, 0.7 mmol) in CH_2Cl_2 (3 mL) to give a colorless solution. In the air, the solvent was removed under reduced pressure and the remaining crystals were washed with diethyl ether (3 × 2 mL) and recrystallized from CH_2Cl_2/diethyl ether at −25 °C to yield 350 mg (70%) of white Pt((*R*,*R*)-*i*-Pr-Duphos)(Ph)(Cl).

Anal. Calcd for $C_{32}H_{49}ClP_2Pt$: C, 52.92; H, 6.80. Found: C, 52.79; H, 6.41. $^{31}P\{^1H\}$ NMR (C_6D_6): δ 58.8 (d, J = 3, J_{Pt-P} = 1627), 47.2 (d, J = 3, J_{Pt-P} = 3944). ^1H NMR (C_6D_6): δ 7.96 (t, J = 7, J_{Pt-H} = 36, 2H), 7.36−7.32 (m, 3H), 7.20−7.16 (m, 1H), 7.10 (t, J = 8, 1H), 7.07−7.00 (m, 2H), 3.38−3.21 (m, 1H), 3.08−3.00 (m, 1H), 2.85−2.76 (m, 1H), 2.55−2.45 (m, 1H), 2.29−2.21 (m, 1H), 2.13−2.03 (m, 2H), 2.02−1.92 (m, 2H), 1.75−1.36 (m, 6H), 1.19 (d, J = 7, 3H, Me), 1.15 (d, J = 7, 3H, Me), 1.12−1.03 (m, 1H), 0.99 (d, J = 7, 3H, Me), 0.91 (d, J = 7, 3H, Me), 0.80 (d, J = 7, 3H, Me), 0.71 (d, J = 7, 3H, Me), 0.64 (d, J = 7, 3H, Me), 0.56 (d, J = 7, 3H, Me). $^{13}C\{^1H\}$ NMR (C_6D_6): δ 161.5 (dd, J = 120, 8, quat, Pt−Ph), 145.3 (dd, J = 45, 38, quat Ar), 144.3 (dd, J = 32, 24, quat Ar), 139.3 (Ph), 133.9 (d, J = 13, Ar), 133.1 (dd, J = 15, 4, Ar), 131.4−131.2 (m, Ar), 131.1−130.9 (m, Ar), 128.6 (d, J = 7, Ph), 123.6 (Ph), 54.7 (d, J = 23, CH), 53.8 (d, J = 38, CH), 48.0 (d, J = 24, CH), 46.6 (d, J = 34, CH), 31.9, 31.7, 31.4, 30.5 (d, J = 8), 30.4 (d, J = 7), 30.0 (d, J = 5), 29.4 (d, J = 2), 28.4 (m), 26.3 (d, J = 7, Me), 26.1 (d, J = 4, Me), 25.5 (d, J = 6, Me), 24.6 (d, J = 6, Me), 22.2 (d, J = 11, Me), 21.9 (d, J = 9, Me), 21.5 (d, J = 6, Me), 21.3 (d, J = 8, Me).

Pt((*R*,*R*)-*i*-Pr-Duphos)(Ph)(PMeIs) (2). PHMe(Is) (112.5 mg, 0.45 mmol) was added with a microsyringe to a stirred slurry of Pt((*R*,*R*)-*i*-Pr-Duphos)(Ph)(Cl) (327 mg, 0.45 mmol) in THF (20 mL). $NaOSiMe_3$ (50.5 mg, 0.45 mmol) in toluene (10 mL) was added to the reaction mixture. The mixture turned yellow immediately. The solvent was removed under vacuum, and toluene (20 mL) was added to the residue. The toluene slurry was filtered through Celite, and the yellow filtrate was concentrated under vacuum. Petroleum ether was added to the yellow residue. The yellow solution was stored at −25 °C for 24 h, yielding yellow crystals suitable for X-ray crystallography, and a yellow solution. The yellow crystals were further washed with petroleum ether (3 × 5 mL) and dried under vacuum, yielding 300 mg (71%) of yellow crystals.

Anal. Calcd for $C_{48}H_{75}P_3Pt$: C, 61.32; H, 8.04. Found: C, 59.14; H, 7.90. Satisfactory analyses for C could not be obtained, perhaps because of the air sensitivity of the complex (Anal. Calcd. for $C_{48}H_{75}P_3PtO$: C, 60.30; H, 7.91). Mass spectroscopy was also consistent with oxidation. HRMS (FAB; *m*/*z*): calcd for $C_{48}H_{76}OP_3Pt^+$ ($M(O)H^+$), 956.4771; found, 956.4668. $^{31}P\{^1H\}$ NMR (21 °C, THF-d_8): δ 54.3 (d, J = 131, J_{Pt-P} = 1654), 50.8 (broad, J_{Pt-P} = 1818), −60.0 (broad). See Table 1 for low-temperature ^{31}P NMR data (four diastereomers). ^1H NMR (THF-d_8): δ 7.88−7.86 (m, 1H, Ar, Duphos), 7.83−7.80 (m, 1H, Ar, Duphos), 7.57 (broad, 1H, Ph ortho), 7.48−7.43 (m, 2H, Ar, Duphos), 7.39 (broad t, J = 7, 1H, J_{Pt-H} = 49, Ph ortho), 6.98 (broad t, J = 8, 1H, Ph meta), 6.94 (broad, 1H, Ph para), 6.90 (2H, Is meta), 6.72 (broad t, J = 8, 1H, Ph meta), 4.68 (broad, 2H, CH, Is), 2.83−2.71 (m, 2H, overlapping CH Duphos + CH Is), 2.70−2.62 (broad, 1H, CH

(29) Pangborn, A. B.; Giardello, M. A.; Grubbs, R. H.; Rosen, R. K.; Timmers, F. J. *Organometallics* **1996**, *15*, 1518−1520.

(30) Clark, H. C.; Manzer, L. E. *J. Organomet. Chem.* **1973**, *59*, 411−428.

(31) Tani, K.; Brown, L. D.; Ahmed, J.; Ibers, J. A.; Nakamura, A.; Otsuka, S.; Yokota, M. *J. Am. Chem. Soc.* **1977**, *99*, 7876−7886.

Duphos), 2.45−2.33 (m, 2H, 2CH Duphos), 2.30−2.16 (broad m, 1H, CH Duphos), 1.99−1.75 (m, 5H, CH + CH_2), 1.75−1.68 (m, 2H, CH_2), 1.64−1.55 (m, 2H, CH_2), 1.49 (qd, J = 13, 5, 2H, CH Duphos), 1.25−1.18 (m, 18H, CH_3), 1.05 (broad, 3H, CH_3), 0.96−0.82 (m, 9H, overlapping CH_3 Duphos and P−Me), 0.68−0.62 (m, 9H, overlapping CH_3), 0.49 (broad, 3H, CH_3), 0.38 (broad, 3H, CH_3). $^{13}C\{^1H\}$ NMR (THF-d_8): δ 161.4 (m, Pt−C, quat Ph), 155.0 (broad, quat Is), 149.0−148.5 (m, quat Duphos), 147.8 (quat Is), 145.2−144.7 (m, quat Duphos), 144.2 (m, quat Is), 140.3 (broad, Ph ortho), 139.2 (Ph ortho), 135.5 (d, J = 15, Ar, Duphos), 134.3 (d, J = 12, Ar, Duphos), 131.3 (m, Ar, Duphos), 130.8 (m, Ar, Duphos), 128.2 (d, J = 6, Ph meta), 127.8 (m, Ph para), 122.2 (Ph meta), 121.1 (Is), 57.2 (d, J = 24, CH, Duphos), 55.9 (d, J = 25, CH, Duphos), 50.1 (broad m, CH, Duphos), 46.1 (d, J = 23, CH Duphos), 35.3 (CH, Is), 33.7 (d, J = 17, CH, Is), 32.5 (CH, Duphos), 31.6 (m, CH, Duphos), 31.1 (d, J = 6, CH_2), 30.9−30.5 (m, CH, Duphos), 30.1−29.8 (m, CH, Duphos), 29.8 (d, J = 8, CH_2), 29.2 (CH_2, Duphos), 27.9 (CH_3), 26.9 (d, J = 4, CH_3), 26.5 (d, J = 2, CH_3), 25.1 (d, J = 6, CH_3), 24.6 (m, CH_3, Is), 22.3 (d, J = 11, CH_3), 22.2 (d, J = 11, CH_3), 21.1 (d, J = 6, CH_3), 20.0 (broad, CH_3), 12.8 (broad m, P−CH_3).

Pt((*R*,*R*)-Me-Duphos)(I)(PMeIs) (3). PHMe(Is) (91 mg, 0.36 mmol) was added with a microsyringe to a stirred slurry of Pt((*R*,*R*)-Me-Duphos)I_2 (275 mg, 0.36 mmol) in toluene (10 mL). $NaOSiMe_3$ (40.8 mg, 0.36 mmol) in toluene (10 mL) was added to the reaction mixture. The mixture turned yellow, and the solution became homogeneous after 10 min. The slurry was filtered through Celite, and the yellow filtrate was concentrated under vacuum. Petroleum ether was added to the yellow residue. The solution was stored at −25 °C for 24 h, yielding yellow crystals suitable for X-ray crystallography and a yellow solution. The yellow crystals were further washed with petroleum ether (3 × 5 mL) and dried under vacuum, yielding 250 mg (78%) of yellow crystals.

HRMS (m/z): calcd for $C_{34}H_{55}IP_3Pt$ (MH^+), 877.2188; found, 877.1935. Anal. Calcd for $C_{34}H_{54}IP_3Pt$: C, 46.53; H, 6.20. Found: C, 35.09; H, 5.19. The poor analytical results presumably stem from decomposition of the air-sensitive sample. $^{31}P\{^1H\}$ NMR (21 °C, toluene-d_8): δ 64.5 (broad d, J = 117, J_{Pt-P} = 1559), 54.4 (broad, J_{Pt-P} = 3943), −68.3 (broad, J_{Pt-P} = 842). See Table 1 for low-temperature ^{31}P NMR data (two diastereomers). ^1H NMR (21 °C, toluene-d_8): δ 7.25−7.19 (m, 1H, Ar), 7.18−7.12 (m, 3H, Ar), 7.08−7.04 (m, 2H, Ar), 5.21 (broad, 2H, CH), 3.97−3.87 (m, 1H, CH), 2.87−2.80 (m, 1H, CH), 2.77−2.60 (broad, 3H), 2.58−2.49 (m, 2H), 2.36 (broad, 1H), 2.22−1.80 (m, 5H), 1.60 (dd, J = 18, 7, 3H, CH_3), 1.48 (d, J = 8, 3H, CH_3), 1.45 (d, J = 7, 6H, $2CH_3$), 1.38 (d, J = 7, 6H, $2CH_3$), 1.29 (d, J = 7, 6H, $2CH_3$), 0.86 (d, J = 7, 3H, CH_3), 0.54 (dd, J = 15, 7, 3H, CH_3), 0.51 (dd, J = 14, 7, 3H, CH_3).

Pt((*R*,*R*)-Me-Duphos)(Cl)(PMeIs) (4). Method I. $NaOSiMe_3$ (34 mg, 0.3 mmol) in toluene (0.5 mL) was added to a stirred slurry of Pt((*R*,*R*)-Me-Duphos)Cl_2 (172 mg, 0.3 mmol) in toluene (1 mL). PHMeIs (75 mg, 0.3 mmol) was added to the reaction mixture, which turned orange immediately. After 2 h, the slurry was filtered through Celite, and the orange filtrate was concentrated under vacuum. The orange residue was washed with petroleum ether (three portions of 0.5 mL), yielding 200 mg (85%) of orange powder. A C_6D_6 solution deposited yellow crystals suitable for X-ray crystallography. The bulk sample contained ∼10% impurities. The major impurity (∼7%), assigned as Pt(Me-Duphos)(OH)(PMeIs), appears to be a mixture of two diastereomers, on the basis of the ^{31}P NMR spectrum (see below). This species was also observed as an impurity in the ^{31}P NMR spectrum of Pt(Me-Duphos)$(PMeIs)_2$ (**5**; see below). Complex **5** was also sometimes seen as an impurity when making **4** via this route.

Method II. A slurry of $NaOSiMe_3$ (13 mg, 0.11 mmol) in toluene (0.5 mL) was added to a slurry of [Pt((*R*,*R*)-Me-Duphos)(Cl)(PHMeIs)][BF_4] (**9**; see below; 100 mg, 0.11 mmol) in toluene (1 mL). The reaction mixture turned yellow immediately. It was filtered through Celite, the filtrate was concentrated under vacuum, and the yellow residue was washed with petroleum ether (three portions of 0.2 mL) and dried under vacuum, yielding 70 mg (78%) of yellow powder. According to ^{31}P NMR spectra, the sample was contaminated with Pt(Me-Duphos)Cl_2, Pt(Me-Duphos)(Cl)($OSiMe_3$) and Pt(Me-Duphos)(OH)(PMeIs) (∼5%). See below for more spectroscopic data for these impurities.

Because complex **4** was not obtained in pure form, we could not get satisfactory elemental analyses for it. Instead, protonation and oxidation gave derivatives **9** and **11** (see below), which were fully characterized. HRMS (m/z): calcd for $C_{34}H_{55}ClOP_3Pt$ (MHO^+), 801.2781; found, 801.2793. $^{31}P\{^1H\}$ NMR (21 °C, THF-d_8): δ 69.5 (broad d, J = 122, J_{Pt-P} = 1605), 53.9 (broad, J_{Pt-P} = 4014), −36.0 (very broad, **b**), −55.0 (broad d, J = 122, J_{Pt-P} = 809, **a**). See Table 1 for low-temperature ^{31}P NMR data (two diastereomers). ^1H NMR (21 °C, THF-d_8): δ 7.86−7.82 (m, 1H, Ar), 7.69−7.63 (m, 1H, Ar), 7.60−7.53 (m, 2H, Ar), 6.96 (2H, Ar), 4.93 (broad, 2H), 3.34−3.23 (m, 1H), 3.05−2.92 (m, 1H), 2.87−2.77 (m, 1H), 2.60−2.46 (m, 1H), 2.40−2.28 (m, 2H), 2.22−2.12 (m, 1H), 2.09−1.95 (m, 1H), 1.95−1.82 (m, 1H), 1.82−1.70 (m, 2H), 1.70−1.60 (m, 1H) overlapping with 1.67 (dd, J = 8, 6, 3H, CH_3), 1.52 (dd, J = 18, 7, 6H, CH_3), 1.26−1.14 (overlapping m, 18H, CH_3), 0.92 (m, 1H), 0.81 (dd, J = 15, 8, 3H, CH_3), 0.56 (broad, 3H, CH_3). ^1H NMR (−20 °C, THF-d_8): δ 7.92−7.87 (m, 1H, Ar), 7.72−7.66 (m, 1H, Ar), 7.65−7.56 (m, 2H, Ar), 6.97 (2H, Ar), 4.93 (broad d, J = 6, 2H, **a**), 4.49 (broad, 2H, **b**), 3.32−3.20 (m, 1H), 3.08−2.92 (m, 1H), 2.88−2.76 (m, 1H), 2.63−2.44 (m, 1H), 2.40−2.27 (m, 2H), 2.20−2.09 (m, 1H), 2.08−1.95 (m, 1H), 1.94−1.82 (m, 2H), 1.83−1.77 (m, 1H), 1.68−1.56 (overlapping m, 4H), 1.56−1.46 (m, 6H, Me), 1.26−1.18 (overlapping m, 12H, Me), 1.16 (d, J = 7, 6H, Me), 0.92−0.85 (m, 1H), 0.80 (dd, J = 15, 7, 3H, Me), 0.53 (dd, J = 16, 7, 3H, Me).

Pt((*R*,*R*)-Me-Duphos)$(PMeIs)_2$ (5). Method I. PHMe(Is) (120 mg, 0.48 mmol) was added with a microsyringe to a stirred slurry of Pt((*R*,*R*)-Me-Duphos)Cl_2 (137 mg, 0.24 mmol) in toluene (1 mL). $NaOSiMe_3$ (53.8 mg, 0.48 mmol) in toluene (1 mL) was added to the reaction mixture. The mixture turned orange, and the solution became homogeneous after 30 min. The slurry was filtered through Celite, and the orange filtrate was concentrated under vacuum. Petroleum ether was added to the yellow residue. The solution was stored at −25 °C for 24 h, yielding yellow crystals suitable for X-ray crystallography and a yellow solution. The yellow crystals were further washed with petroleum ether (3 × 1 mL) and dried under vacuum, yielding 195 mg (81%) of yellow crystals. On the basis of the ^{31}P NMR spectra, the sample was contaminated with Pt((*R*,*R*)-Me-Duphos)(Cl)(PMeIs) (**4**), Pt((*R*,*R*)-Me-Duphos)($OSiMe_3$)(PMeIs), Pt((*R*,*R*)-Me-Duphos)(OH)(PMeIs), PHMe(Is), and other unidentified impurities (∼10% total, see below).

Method II. To a slurry of [Pt((*R*,*R*)-Me-Duphos)$(PHMeIs)_2$][$OTf]_2$ (**10**; see below; 70 mg, 0.054 mmol) in toluene (1 mL) was added a slurry of $NaOSiMe_3$ (12 mg, 0.11 mmol) in toluene (1 mL). The reaction mixture turned yellow immediately. It was filtered through Celite, and the filtrate was concentrated under vacuum. The viscous residue was washed with petroleum ether (3 × 0.5 mL) and dried under vacuum, yielding 45 mg (82%) of yellow powder. On the basis of the ^{31}P NMR spectra, the sample was contaminated with Pt((*R*,*R*)-Me-Duphos)(Cl)(PMeIs) (**4**), PHMe(Is), and other unidentified impurities (∼10% total).

We could not obtain spectroscopically pure bulk samples of **5**, although it could be characterized crystallographically. Satisfactory elemental analyses could not be obtained for this material, perhaps because of its air sensitivity. Anal. Calcd for $C_{50}H_{80}P_4Pt$: C, 60.04; H, 8.06. Found: C, 58.32; H, 8.11. These results are consistent with oxidation at both phosphorus centers: Anal. Calcd for $C_{50}H_{80}O_2P_4Pt$: C, 58.18; H, 7.81. Mass spectroscopy was also

consistent with oxidation. HRMS (*m*/*z*): calcd for $C_{50}H_{81}P_4PtO_2$ $(MO_2H)^+$, 1032.4849; found, 1032.4847. $^{31}P\{^1H\}$ NMR (21 °C, THF-d_8): δ 57.5 (broad), −56.7 (broad). See Table 1 for low-temperature ^{31}P NMR data. In addition to the three diastereomers listed there, we consistently observed PHMe(Is) and a trace amount of an unidentified phosphido complex ($^{31}P\{^1H\}$ NMR (−50 °C, THF-d_8): δ 57.8 (apparent dd, J = 114, 12), −102.9 (apparent dd, J = 114, 12, J_{Pt-P} = 894)) in bulk samples of **5**. We cannot exclude the possibility that these peaks are due to a fourth diastereomer of **5**; they could also simply result from an impurity. ^1H NMR (21 °C, THF-d_8): δ 7.82−7.74 (m, 2H, Ar), 7.54−7.48 (m, 2H, Ar), 6.92 (broad, 4H, Ar), 5.00 (broad, 4H, CH), 2.87−2.72 (m, 4H), 2.65−2.35 (broad, 2H), 2.28−2.10 (m, 2H), 2.10−1.70 (m, 6H), 1.62−1.54 (m, 12H, Me), 1.26−1.13 (overlapping m, 36H, CH_3), 0.55 (dd, J = 25, 12, 6H, CH_3).

Intermediates and Impurities in the Formation of Phosphido Complexes 4 and 5. To investigate the formation of complexes **4** and **5**, we studied the reaction of the chloro complexes Pt((*R*,*R*)-Me-Duphos)Cl_2 and Pt((*R*,*R*)-Me-Duphos)(Cl)(PMeIs) (**4**) with $NaOSiMe_3$, followed by the addition of PHMe(Is). Several complexes were observed by ^{31}P NMR spectroscopy; NMR data and tentative assignments are included below. To account for all the observations, including the magnitude of the J_{Pt-P} coupling constants, we have assigned some species as platinum hydroxides, assuming that they form via Me_3SiOH, which decomposes to water and $(Me_3Si)_2O$, and/or from adventitious water. The complicated nature of the reaction mixtures is consistent with the difficulty we observed in isolating pure **4** or **5** by these routes.

Reaction of Pt((*R*,*R*)-Me-Duphos)Cl_2 with 2 Equiv of $NaOSiMe_3$. To a white slurry of Pt((*R*,*R*)-Me-Duphos)Cl_2 (40 mg, 0.07 mmol) in THF (0.2 mL) was added a slurry of $NaOSiMe_3$ (16 mg, 0.14 mmol, 2 equiv) in 0.3 mL of THF. The reaction mixture was transferred to an NMR tube and monitored by ^{31}P NMR spectroscopy. After 10 min a white precipitate was still observed on the bottom of the tube, and unreacted Pt((*R*,*R*)-Me-Duphos)Cl_2 (12% of the mixture by ^{31}P NMR integration) was observed in the solution. The major component (65%) of the solution was tentatively assigned as Pt((*R*,*R*)-Me-Duphos)(Cl)($OSiMe_3$); 23% of the material was another unsymmetrical Pt(Duphos) complex, perhaps Pt((*R*,*R*)-Me-Duphos)(OH)($OSiMe_3$).

Pt((*R*,*R*)-Me-Duphos)(Cl)($OSiMe_3$). $^{31}P\{^1H\}$ NMR (21 °C, THF): δ 65.6 (d, J = 7, J_{Pt-P} = 3801), 55.5 (d, J = 7, J_{Pt-P} = 3289).

Pt((*R*,*R*)-Me-Duphos)(OH)($OSiMe_3$). $^{31}P\{^1H\}$ NMR (21 °C, THF): δ 55.9 (d, J = 10, J_{Pt-P} = 3635), 54.4 (d, J = 10, J_{Pt-P} = 3115).

Addition of 1 Equiv of PHMe(Is). The above mixture was added to PHMe(Is) (18 mg, 0.07 mmol). The color changed to orange immediately. It was transferred to an NMR tube and monitored by ^{31}P NMR spectroscopy. After 10 min precipitate was still observed. Unreacted PHMe(Is) was a major component of the mixture. The Pt(Duphos) species in solution were Pt((*R*,*R*)-Me-Duphos)(Cl)(PMeIs) (**4**; 55%), Pt((*R*,*R*)-Me-Duphos)($OSiMe_3$)(PMeIs) (21%), Pt((*R*,*R*)-Me-Duphos)(OH)($OSiMe_3$) (13%), Pt((*R*,*R*)-Me-Duphos)(Cl)($OSiMe_3$) (6%), and two other unidentified species, one possibly Pt((*R*,*R*)-Me-Duphos)(OH)(PMeIs) (3%) and the other Pt((*R*,*R*)-Me-Duphos)X_2 (X = $OSiMe_3$ or OH) (1%). After 20 h, PHMe(Is) was entirely consumed, and the Pt(Duphos) species in solution were **4** (50%), Pt((*R*,*R*)-Me-Duphos)(OH)(PMeIs) (25%), Pt((*R*,*R*)-Me-Duphos)(OH)($OSiMe_3$) (10%), Pt((*R*,*R*)-Me-Duphos)($OSiMe_3$)$_2$ (10%), Pt((*R*,*R*)-Me-Duphos)(Cl)($OSiMe_3$) (3%), and Pt((*R*,*R*)-Me-Duphos)($OSiMe_3$)(PMeIs) (2%).

Pt((*R*,*R*)-Me-Duphos)($OSiMe_3$)(PMeIs). $^{31}P\{^1H\}$ NMR (21 °C, THF): δ 66.8 (dd, J = 136, 10, J_{Pt-P} = 1620), 43.5 (J_{Pt-P} = 3815), −44.8 (broad d, J = 136, J_{Pt-P} ≈ 800).

Pt((*R*,*R*)-Me-Duphos)X_2 (X = $OSiMe_3$, OH). $^{31}P\{^1H\}$ NMR (21 °C, THF): δ 54.7 (J_{Pt-P} = 3545).

Pt((*R*,*R*)-Me-Duphos)(OH)(PMeIs). $^{31}P\{^1H\}$ NMR (21 °C, THF-d_8): δ 70.5 (dd, J = 151, 8, J_{Pt-P} = 1857), 49.4 (broad, J_{Pt-P} ∼3300), −44.9 (broad). At low temperature, a 1:1 mixture of diastereomers was observed. $^{31}P\{^1H\}$ NMR (−20 °C, THF-d_8): δ 70.5 (dd, J = 152, 8, J_{Pt-P} ≈ 1860), overlapping with 70.4 (dd, J ≈ 150, 5), 52.5 (J_{Pt-P} ≈ 3174), 48.8 (J_{Pt-P} ≈ 3226), −41.9 (d, J = 151), −44.5 (d, J ≈ 150).

Addition of 1 Equiv More of PHMe(Is). The above mixture was added to PHMe(Is) (18 mg, 0.07 mmol). It was transferred to an NMR tube and monitored by ^{31}P NMR spectroscopy. After 3 h a precipitate was observed. Unreacted PHMe(Is) was a major component of the mixture. The Pt(Duphos) species in solution were Pt((*R*,*R*)-Me-Duphos)(PMeIs)$_2$ (**5**; 61%), Pt((*R*,*R*)-Me-Duphos)(OH)(PMeIs) (24%), Pt((*R*,*R*)-Me-Duphos)(Cl)(PMeIs) (**4**; 6%), Pt((*R*,*R*)-Me-Duphos)($OSiMe_3$)(PMeIs) (3%), Pt((*R*,*R*)-Me-Duphos)($OSiMe_3$)$_2$ (3%), and Pt((*R*,*R*)-Me-Duphos)(OH)($OSiMe_3$) (3%). After 20 h a precipitate was observed. Unreacted PHMeIs was a major component of the mixture. The Pt(Duphos) species in solution were **5** (69%), Pt((*R*,*R*)-Me-Duphos)(OH)(PMeIs) (29%), and Pt((*R*,*R*)-Me-Duphos)($OSiMe_3$)(PMeIs) (2%).

Reaction of Pt((*R*,*R*)-Me-Duphos)(Cl)(PMeIs) with $NaOSiMe_3$/PHMeIs. To a solution of Pt((*R*,*R*)-Me-Duphos)(Cl)(PMeIs) (**4**; contaminated with ∼7% impurity assigned as Pt((*R*,*R*)-Me-Duphos)(OH)(PMeIs); 55 mg, 0.07 mmol) in THF (0.2 mL) was added a slurry of $NaOSiMe_3$ (8 mg, 0.07 mmol) in 0.3 mL of THF. The mixture was transferred to an NMR tube and monitored by ^{31}P NMR spectroscopy; after 3 h, no reaction had occurred. The mixture was added to PHMe(Is) (18 mg, 0.07 mmol), transferred to an NMR tube, and monitored by ^{31}P NMR spectroscopy. After 30 min the mixture was unchanged. After 20 h the mixture consisted mainly of Pt((*R*,*R*)-Me-Duphos)(PMeIs)$_2$ (**5**), along with unreacted PHMe(Is) and Pt((*R*,*R*)-Me-Duphos)(OH)(PMeIs).

[**Pt((*R*,*R*)-Me-Duphos)(Ph)(PHMe(Is))][BF_4] (6). Method I.** To a stirred solution of Pt((*R*,*R*)-Me-Duphos)(Ph)(PMeIs) (**1**; 64 mg, 0.08 mmol) in Et_2O (10 mL) was added HBF_4·Me_2O (12 mg, 0.085 mmol). A white precipitate formed immediately. After it settled, the solvent was removed with a pipet and the precipitate was washed with Et_2O (3 × 5 mL). The precipitate was dried under vacuum, yielding 55 mg (75%) of white powder. The ^{31}P NMR spectrum is reported for a mixture of two diastereomers **a** and **b**, whose ratio varied over time (ratio **a**:**b** = 5:1 after 1 h, 14:1 after 1 day).

Anal. Calcd for $C_{40}H_{60}P_3PtBF_4$: C, 52.47; H, 6.60. Found: C, 52.09; H, 6.66. $^{31}P\{^1H\}$ NMR (CD_2Cl_2): diastereomer **a**, δ 63.1 (dd, J = 372, 8, J_{Pt-P} = 2623), 62.8 (dd, J = 18, 8, J_{Pt-P} = 1643), −62.6 (dd, J = 372, 18, J_{Pt-P} = 2513); diastereomer **b**, δ 61.4 (dd, J = 376, 6, J_{Pt-P} = 2618), 67.6 (m, J_{Pt-P} = 1691), −55.2 (dd, J = 376, 18, J_{Pt-P} = 2472). Selected ^1H NMR data (CD_2Cl_2, all for the major diastereomer **a** unless indicated): δ 7.24 (dm, J = 355, P−H, **b**), 7.21 (d, J = 4, 2H, Is), 6.79 (dm, J = 361, P−H), 1.45 (dd, J = 19, 7, 3H, CH_3, Duphos), 1.36 (dd, J = 18, 8, 3H, CH_3, Duphos), 1.35 (d, J = 7, 6H, $2CH_3$ Is), 1.29 (d, J = 7, 6H, $2CH_3$, Is), 1.26 (d, J = 7, 6H, $2CH_3$, Is), 1.08 (ddd, J = 7, 4, 2, J_{Pt-H} = 38, P−CH_3), 0.87 (dd, J = 17, 8, 3H, CH_3, Duphos), 0.74 (m, 1H, CH, Duphos), 0.69 (dd, J = 16, 7, 3H, CH_3, Duphos).

Method II. To a stirred solution of Pt((*R*,*R*)-Me-Duphos)(Ph)(Cl) (140 mg, 0.22 mmol) and PHMe(Is) (21 mg, 0.22 mmol) in THF (20 mL) was added AgOTf (57.1 mg, 0.22 mmol) dissolved in THF (5 mL). Immediate formation of AgCl was observed, and the reaction mixture was stirred vigorously at room temperature for 30 min and then filtered through Celite and concentrated under vacuum. Petroleum ether was added to the viscous residue, and cooling of this solution to −25 °C gave 167 mg (77%) of an off-white solid, **6-OTf**.

[**Pt((*R*,*R*)-*i*-Pr-Duphos)(Ph)(PHMe(Is))][BF_4] (7).** A solution of HBF_4·Me_2O (11.6 mg, 0.086 mmol) in 10 mL of Et_2O was added to a yellow solution of Pt((*R*,*R*)-*i*-Pr-Duphos)(Ph)(PMeIs) (**2**; 74 mg, 0.08 mmol) in 10 mL of Et_2O. A white precipitate formed

immediately. The solvent was removed with a pipet, and the precipitate was washed with Et_2O (3 portions of 5 mL) and then dried under vacuum, yielding 55 mg (67%) of the product as a 1.3:1 mixture of the two diastereomers **a** and **b**. Recrystallization from THF/petroleum ether yielded crystals of diastereomer **a**, as shown by NMR spectroscopy in CD_2Cl_2. The solvent was removed from this sample under vacuum to give a solid which was analyzed correctly for a CD_2Cl_2 solvate.

Anal. Calcd for $C_{48}H_{76}P_3PtBF_4 \cdot CD_2Cl_2$: C, 52.79; H, 6.87. Found: C, 52.74; H, 7.16. From comparison of the NMR spectra of the 1.3:1 mixture and pure diastereomer **a**, assignments of most of the NMR signals could be made. $^{31}P\{^1H\}$ NMR (CD_2Cl_2): diastereomer **a**, δ 58.4 (dd, $J = 372$, 6, $J_{Pt-P} = 2681$), 57.3 (dd, $J = 17$, 6, $J_{Pt-P} = 1656$), −66.1 (dd, $J = 372$, 17, $J_{Pt-P} = 2510$); diastereomer **b**, δ 57.1 (dd, $J = 377$, 5, $J_{Pt-P} = 2687$), 53.7 (dd, $J = 15$, 5, $J_{Pt-P} = 1631$), −60.3 (dd, $J = 377$, 15, $J_{Pt-P} = 2481$). ^1H NMR (diastereomer **a**, CD_2Cl_2): δ 7.85−7.80 (m, 1H, Ar), 7.77−7.74 (m, 1H, Ar), 7.74−7.66 (m, 2H, Ar), 7.65−7.50 (t, $J = 6$, $J_{Pt-H} = 41$, 1H, Ar), 7.31−7.24 (m, 3H, Ar), 7.18 (d, $J = 3$, 2H, Ar), 7.12−7.02 (m, 1H, Ar), 6.76 (dm, $J = 358$, 1H, PH), 3.52−3.50 (m, 2H, *i*-Pr CH), 2.94−2.89 (m, 1H), 2.74−2.51 (m, 5H), 2.09−1.83 (m, 5H), 1.71−1.66 (m, 1H), 1.60−1.44 (m, 5H), 1.33−1.28 (overlapping m, 15H), 1.23 (overlapping d, $J = 7$, 6H), 1.12−1.07 (m, 3H, P−Me), 1.03 (d, $J = 6$, 3H), 0.76 (d, $J = 6$, 3H), 0.64 (d, $J = 6$, 3H), 0.56 (d, $J = 6$, 3H), 0.30 (d, $J = 6$, 3H), 0.18 (d, $J = 6$, 3H). ^1H NMR (selected signals for diastereomer **b**, CD_2Cl_2; in some cases, overlap with signals from **a** precluded assignment): δ 7.93−7.91 (m, 1H, Ar), 7.82−7.72 (m, overlapping signals from major diastereomer, 2H, Ar), 7.01 (broad, 2H, Ar), 6.86−6.84 (m, 2H, Ar), 6.74−6.71 (m, 1H, Ar), 6.44 (dm, $J = 372$, 1H, PH), 1.36−1.28 (m, overlapping signals from major diastereomer, 9H), 1.23 (d, $J = 7$, 6H), 1.14−1.08 (m, overlapping signals from major diastereomer, 9H), 0.99 (d, $J = 7$, 3H), 0.89 (d, $J = 6$, 3H), 0.87 (d, $J = 6$, 3H), 0.78 (d, $J = 7$, 3H), 0.71 (d, $J = 6$, 3H), 0.70 (d, $J = 6$, 3H), 0.58 (d, $J = 6$, 3H).

[Pt((*R*,*R*)-Me-Duphos)(I)(PH(Me)(Is))][BF$_4$] (8). To a stirred solution of Pt((*R*,*R*)-Me-Duphos)(I)(PMeIs) (88 mg, 0.1 mmol) in Et_2O (10 mL) was added $HBF_4 \cdot Me_2O$ (16 mg, 12.5 μL, 0.12 mmol). An off-white precipitate formed immediately. After it settled, the solvent was removed with a pipet and the precipitate was washed with Et_2O (3 × 5 mL). The precipitate was dried under vacuum, yielding 85 mg (88%) of off-white powder, which was recrystallized from CH_2Cl_2/Et_2O for elemental analyses. Note: this and the related cationic secondary phosphine complexes tended to cocrystallize with these solvents, which were readily lost on standing. In this case, a trace of CH_2Cl_2 was observed by ^1H NMR spectroscopy in the analytical sample. Anal. Calcd for $BC_{34}F_4H_{55}IP_3Pt$: C, 42.30; H, 5.74. Anal. Calcd for $BC_{34}F_4H_{55}IP_3Pt \cdot 0.05CH_2Cl_2$ (observed by ^1H NMR (CD_2Cl_2)): C, 42.17; H, 5.73. Found: C, 41.77; H, 5.80.

The NMR spectra are reported for a mixture of two diastereomers (ratio **a**:**b** = 3:1 on the basis of integration of the ^1H NMR spectrum). $^{31}P\{^1H\}$ NMR (CD_2Cl_2): diastereomer **a**, δ 74.8 (d, $J = 374$, $J_{Pt-P} = 2321$), 65.0 (d, $J = 18$, $J_{Pt-P} = 3102$), −72.0 (dd, $J = 374$, 18, $J_{Pt-P} = 2213$); diastereomer **b**, δ 73.4 (d, $J = 383$, $J_{Pt-P} = 2289$), 72.0 (d, $J = 15$, $J_{Pt-P} = 3175$), −65.8 (dd, $J = 383$, 15, $J_{Pt-P} = 2164$). ^1H NMR (CD_2Cl_2): δ 7.92−7.76 (m, 3H), 7.73 (tm, $J = 7$, 1H), 7.22 (d, $J = 4$, 2H, Is, **a**), 7.16 (d, $J = 4$, 2H, Is, **b**), 6.67 (dm, $J = 384$, P−H, **b**), 6.43 (dm, $J = 343$, P−H, **a**), 4.06−3.93 (m, 1H, **a**), 3.88−3.78 (m, 1H), 3.62−3.54 (m, 1H, **b**), 3.12−2.79 (m, 2H), 2.63−2.23 (m, 5H), 2.23−2.08 (m, 1H, **a**), 2.08−1.78 (m, 2H), 1.78−1.66 (m, 1H, **b**), 1.54 (d, $J = 7$, 3H, **a**), 1.53 (dd, $J = 20$, 7, 3H, **a**, overlapping 3H, **b**), 1.43−1.33 (m, 4H), 1.33−1.24 (m, 18H), 1.12 (dd, $J = 7$, 3, 3H, **b**), 1.09 (d, $J = 7$, 3H, b), 0.90−0.82 (m, 3H), 0.69 (dd, $J = 17$, 7, 3H, **a**).

[Pt((*R*,*R*)-Me-Duphos)(Cl)(PHMe(Is))][BF$_4$] (9). Method I. To a stirred yellow slurry of Pt((*R*,*R*)-Me-Duphos)(Cl)(PMeIs) (**4**; 79 mg, 0.1 mmol) in Et_2O (2 mL) was added $HBF_4 \cdot Me_2O$ (26 mg, 12.5 μL, 0.12 mmol). An off-white slurry formed immediately, and the solvent was removed under vacuum. Petroleum ether (1 mL) was added to the viscous residue, and an off-white precipitate formed. The solvent was removed with a pipet, and the precipitate was washed with petroleum ether (3 × 2 mL). The precipitate was dried under vacuum, yielding 76 mg (87%) of white powder. The ^1H NMR spectrum is reported as a mixture of two diastereomers (ratio **a**:**b** = 2.3:1 based on integration of P−H signals) unless otherwise indicated. Because the starting material was not pure, we could not obtain the cation in pure form (∼5% of unidentified impurities).

Method II. A slurry of $AgBF_4$ (39 mg, 0.2 mmol) in CH_3CN (0.5 mL) was added to a slurry of Pt((*R*,*R*)-Me-Duphos)Cl_2 (115 mg, 0.2 mmol) in CH_3CN (1 mL), with stirring. A white precipitate formed immediately. The mixture was filtered through Celite and concentrated under vacuum. The ^{31}P NMR (CH_3CN) spectrum of the solution showed the presence of ∼10% of impurities (unreacted Pt((*R*,*R*)-Me-Duphos)Cl_2 and [Pt((*R*,*R*)-Me-Duphos)-$(NCMe)_2$][BF_4]$_2$). The solvent was removed under vacuum, and the residue was washed with petroleum ether (3 × 0.2 mL) and dried under vacuum. Recrystallization from THF/petroleum ether yielded 110 mg (76%) of white powder, which was used in the next step without further purification.

[Pt((*R*,*R*)-Me-Duphos)(Cl)(NCMe)][BF$_4$]. $^{31}P\{^1H\}$ NMR (CD_2Cl_2): δ 70.9 ($J_{Pt-P} = 3307$), 64.5 ($J_{Pt-P} = 3664$). $^{31}P\{^1H\}$ NMR (CH_3CN): δ 70.7 ($J_{Pt-P} = 3300$), 64.4 ($J_{Pt-P} = 3645$).

[Pt((*R*,*R*)-Me-Duphos)(NCMe)$_2$][BF$_4$]$_2$. This complex was generated independently, using 2 equiv of $AgBF_4$. $^{31}P\{^1H\}$ NMR (CD_2Cl_2): δ 67.3 ($J_{Pt-P} = 3478$). $^{31}P\{^1H\}$ NMR (CH_3CN): δ 67.0 ($J_{Pt-P} = 3495$).

Pt((*R*,*R*)-Me-Duphos)Cl$_2$. $^{31}P\{^1H\}$ NMR (CD_2Cl_2): δ 69.4 ($J_{Pt-P} = 3557$). $^{31}P\{^1H\}$ NMR (CH_3CN): δ 68.1 ($J_{Pt-P} = 3511$).

A solution of PHMe(Is) (41.5 mg, 0.165 mmol) in CH_2Cl_2 (0.5 mL) was added to a solution of impure [Pt((*R*,*R*)-Me-Duphos)-(Cl)(NCMe)][BF_4] (110 mg, 0.165 mmol) in CH_2Cl_2 (1 mL). The solvent was removed under vacuum, and the white residue was washed with petroleum ether (3 × 0.5 mL) and dried under vacuum, yielding 105 mg (73%) of white powder. CH_2Cl_2 (0.2 mL) was added to the powder, and crystals suitable for X-ray crystallography were formed on the walls of the vial. The solvent was removed with a pipet, and the crystals were dried under vacuum. The compound was found to cocrystallize with CH_2Cl_2 by X-ray crystallography and elemental analyses. Two diastereomers were observed (ratio **a**:**b** = 1:1.4 on the basis of integration of P−H signals in the ^1H NMR spectrum). Impurities (Pt((*R*,*R*)-Me-Duphos)Cl_2 and an unidentified Pt−secondary phosphine species (perhaps (Pt((*R*,*R*)-Me-Duphos)(PHMe(Is))(NCMe)][BF_4]$_2$, ∼5%)) were still observed in the ^{31}P NMR spectrum of the bulk material.

Anal. Calcd. for $BC_{34}F_4H_{55}ClP_3Pt$: C, 46.72; H, 6.34. Calcd for $BC_{34}F_4H_{55}ClP_3Pt \cdot 0.4CH_2Cl_2$: C, 45.50; H, 6.19. Found: C, 45.25; H, 5.79. HRMS (*m*/*z*): calcd for $C_{34}ClH_{55}P_3Pt^+$ (M^+), 785.2832; found, 785.2837. $^{31}P\{^1H\}$ NMR (CD_2Cl_2): diastereomer **a**, δ 78.9 (dd, $J = 377$, 3, $J_{Pt-P} = 2380$), 62.9 (dd, $J = 18$, 3, $J_{Pt-P} = 3282$), −60.3 (dd, $J = 377$, 18, $J_{Pt-P} = 2227$); diastereomer **b**, δ 78.8 (dd, $J = 379$, 3, $J_{Pt-P} = 2356$), 65.4 (d, $J = 17$, $J_{Pt-P} = 3312$), −53.5 (dd, $J = 379$, 17, $J_{Pt-P} = 2230$). ^1H NMR (CD_2Cl_2): δ 7.84−7.70 (m, 3H), 7.70−7.64 (m, 1H), 7.22 (d, $J = 4$, 2H, Is, **a**), 7.18 (d, $J = 4$, 2H, Is, **b**), 6.44 (dm, $J = 362$, P−H, **a**), 6.29 (dm, $J = 371$, P−H, **b**), 3.86−3.76 (m, 2H, **a**), 3.68−3.62 (m, 2H, **b**), 3.44−3.31 (m, 1H), 3.15−2.76 (m, 3H), 2.58−2.26 (m, 4H), 2.26−2.12 (m, 1H), 2.06−1.98 (m, 3H, Me), 1.96−1.68 (m, 4H), 1.54 (dd, $J = 20$, 7, 3H, Me, **a**), 1.58−1.23 (overlapping m, 21H, Me), 1.05 (dd, $J = 17$, 7, 3H, **b**), 0.96−0.82 (m, 3H, Me), 0.69 (dd, $J = 17$, 7, 3H, **a**), 0.66 (dd, $J = 20$, 8, 3H, Me, **b**). NMR data for the unidentified impurity: $^{31}P\{^1H\}$ NMR (CD_2Cl_2) δ 80.3 (d, $J = 380$), 67.1 (d, $J = 17$), −82.8 (dd, $J = 377$, 17).

[Pt((*R*,*R*)-Me-Duphos)(PHMe(Is))$_2$][BF$_4$]$_2$ (10). To a stirred solution of Pt((*R*,*R*)-Me-Duphos)$(PMeIs)_2$ containing ∼30% of

chloro complex **4** impurity (100 mg, 0.1 mmol) in Et_2O (10 mL) was added $HBF_4{\cdot}Me_2O$ (32 mg, 25 μL, 0.24 mmol). A white precipitate formed immediately. After it settled, the solvent was removed with a pipet and the precipitate was washed with Et_2O (3 × 5 mL). The precipitate was dried under vacuum, yielding 115 mg (98%) of white powder, whose ^{31}P NMR spectrum showed that it consisted of a mixture of dication **10** (~70%) and cation **9** (~30%). Recrystallization from CH_2Cl_2/Et_2O yielded white crystals of a methylene chloride solvate of **10** as a mixture of three diastereomers (ratio **a**:**b**:**c** = 3.7:1.2:1, from ^1H NMR integration). Anal. Calcd for $C_{50}H_{82}P_4PtB_2F_8$: C, 51.08; H, 7.03. Anal. Calcd. for $C_{50}H_{82}P_4PtB_2F_8{\cdot}CH_2Cl_2$: C, 48.59; H, 6.72. Found: C, 48.60; H, 6.97. The cocrystallized solvent was observed by ^1H NMR spectroscopy in CD_2Cl_2. HRMS (*m*/*z*): calcd for $C_{50}H_{83}P_4Pt$ $(MH)^{3+}$, 1001.5072; found, 1001.4654. $^{31}P\{^1H\}$ NMR (CD_2Cl_4): diastereomer **a**, δ 70.7 (AA′XX′ pattern, $J_{AX} = 297$, $J_{AX'} = -23$, $J_{AA'} = 31$, $J_{XX'} = 0$, $J_{Pt-P} = 2188$), −71.6 (AA′XX′ pattern, $J_{AX} = 297$, $J_{AX'} = -23$, $J_{AA'} = 31$, $J_{XX'} = 0$, $J_{Pt-P} = 2202$); other diastereomers, δ 77.9 (broad d, $J = 294$), 68.5 (apparent dd, $J = 296$, 23, $J_{Pt-P} = 2150$), −67.9 (broad), −69.4 (broad). Selected ^1H NMR (CD_2Cl_4) signals: 8.00−7.80 (m, 4H, Ar), 7.36−7.30 (broad, 4H, Is, **a**), 7.30−7.24 (broad m, 4H, Is, **b**), 7.24−7.20 (broad m, 4H, Is, **c**), 7.18 (broad dm, $J_{P-H} = 383$, 2H, P−H, **b**), 7.12 (broad dm, $J_{P-H} = 383$, 2H, P−H, **a**), 6.72 (broad dm, $J_{P-H} = 388$, 2H, P−H, **c**), 3.62−3.53 (m, 2H), 3.44−3.20 (m, 2H), 3.15−2.96 (m, 2H), 2.80−2.62 (m, 2H), 2.46−2.30 (m, 4H), 2.28−1.90 (m, 4H), 1.70−1.28 (overlapping m, ~51H, Me), 1.02 (dd, $J = 18$, 7, 3H, Me, **b**), 0.75 (dd, $J = 17$, 7, 3H, Me, **a**), 0.62 (dd, $J = 18$, 7, 3H, Me, **c**).

[Pt((*R*,*R*)-Me-Duphos)(PHMe(Is))$_2$][OTf]$_2$ (10-OTf). A solution of PHMe(Is) (69 mg, 0.28 mmol) in CH_2Cl_2 (0.5 mL) was added to a solution of Pt((*R*,*R*)-Me-Duphos)$(OTf)_2$ (110 mg, 0.138 mmol, see below) in CH_2Cl_2 (1 mL). The solvent was removed under vacuum, and THF (0.3 mL) was added to the mixture. After a few minutes white crystals started to precipitate. The solution was removed with a pipet, and the crystals were washed with THF (3 × 0.2 mL) and dried under vacuum, yielding 75 mg (43%) of white crystals as a mixture of 3 diastereomers (ratio **a**:**b**:**c** = 3.8:1:1.1).

$^{31}P\{^1H\}$ NMR (CD_2Cl_2): diastereomer **a**, δ 69.9 (AA′XX′ pattern, $J_{AX} = 298$, $J_{AX'} = -24$, $J_{AA'} = 32$, $J_{XX'} = 0$, $J_{Pt-P} = 2188$), −71.6 (AA′XX′ pattern, $J_{AX} = 298$, $J_{AX'} = -24$, $J_{AA'} = 32$, $J_{XX'} = 0$, $J_{Pt-P} = 2200$); diastereomer **b**, δ 78.2 (dd, $J = 289$, 19, $J_{Pt-P} = 2275$), −68.0 (broad d, $J = 310$, $J_{Pt-P} = 2237$), diastereomer **c**, δ 68.1 (apparent dd, $J = 296$, 24, $J_{Pt-P} = 2158$), −70.9 (broad d, $J = 287$, $J_{Pt-P} = 2160$).

Pt((*R*,*R*)-Me-Duphos)$(OTf)_2$. To a slurry of Pt((*R*,*R*)-Me-Duphos)Cl_2 (115 mg, 0.2 mmol) in CH_2Cl_2 (1 mL) was added a slurry of AgOTf (103 mg, 0.4 mmol) in CH_2Cl_2 (1 mL). A white precipitate formed immediately. The slurry was filtered through Celite, and the filtrate was concentrated under vacuum. The ^{31}P NMR spectrum of the filtrate indicated only ~65% conversion. A slurry of AgOTf (55 mg, 0.2 mmol) in CH_2Cl_2 (1 mL) was added to the filtrate. A gray precipitate was observed after 15 h. The mixture was filtered through Celite, and the filtrate was concentrated under vacuum. The white residue was washed with petroleum ether (3 × 0.5 mL) and dried under vacuum, yielding 120 mg (75% yield) of white powder.

Anal. Calcd for $C_{20}H_{28}F_6O_6P_2PtS_2$: C, 30.04; H, 3.53. Found: C, 30.21; H, 3.65. $^{31}P\{^1H\}$ NMR (CD_2Cl_2): δ 65.9 ($J_{Pt-P} = 4038$). ^1H NMR (CD_2Cl_2): δ 7.85−7.70 (m, 4H, Ar), 3.75−3.55 (m, 2H), 2.82−2.64 (m, 2H), 2.50−2.25 (m, 4H), 2.10−1.90 (m, 2H), 1.88−1.70 (m, 2H), 1.52 (dd, $J = 20$, 7, 6H, Me), 0.87 (dd, $J = 18$, 7, 6H, Me). $^{13}C\{^1H\}$ NMR (CD_2Cl_2): δ 137.6 (dd, $J = 60$, 21, quat), 134.2−134.1 (m, Ar), 133.4−132.1 (m, Ar), 120.2 (q, $J_{C-F} = 319$, OSO_2CF_3), 40.4 (d, $J = 40$, $J_{Pt-C} = 30$, CH), 36.6 (d, $J = 38$, $J_{Pt-C} = 33$, CH), 36.3 ($J_{Pt-C} = 35$, CH_2), 34.6 (broad two-line pattern with apparent $J = 7$, CH_2), 16.8 ($J_{Pt-C} = 35$, Me), 13.5 (Me).

Pt((*R*,*R*)-Me-Duphos)(Cl)(P(O)MeIs) (11). Method I. To a yellow solution of impure Pt((*R*,*R*)-Me-Duphos)(Cl)(PMeIs) (**4**; 70 mg, 0.09 mmol) in 0.5 mL of THF-d_8 in an NMR tube fitted with a rubber septum was added H_2O_2 (30% in H_2O, 20 μL, 0.18 mmol), with a microliter syringe. The reaction mixture became colorless, and gas evolved. ^{31}P NMR spectroscopy indicated the formation of **11**. The solvent was removed under vacuum, and the white residue was washed with ether (3 × 0.5 mL). Drying the precipitate yielded 68 mg (94%) of white powder as a mixture of two diastereomers (ratio **a**:**b** = 10.8:1). Recrystallization from CD_2Cl_2/ether at 5 °C gave crystals enriched in diastereomer **a** (ratio **a**:**b** = 28.1:1).

Method II. A yellow solution of Pt((*R*,*R*)-Me-Duphos)(Cl)(PMeIs) (**4**; 50 mg, 0.06 mmol) in 0.5 mL of toluene-d_8 in a capped, Parafilm-wrapped NMR tube became colorless after 2 months in the air. Crystals suitable for X-ray crystallography formed on the walls of the NMR tube.

HRMS (*m*/*z*): calcd for $C_{34}H_{54}ClOP_3Pt^+$ (M^+), 801.2737; found, 801.2780. Anal. Calcd for $C_{34}H_{54}OClP_3Pt$: C, 50.90; H, 6.78. Calcd for $C_{34}H_{54}OClP_3Pt{\cdot}0.5CD_2Cl_2$ (the solvent of recrystallization): C, 49.00; H, 6.44. Found: C, 48.78; H, 6.66. $^{31}P\{^1H\}$ NMR (CD_2Cl_2): diastereomer **a**, δ 64.9 (collapsed[32] dd, $J = 431$, 9, $J_{Pt-P} = 1452$), 64.7 (collapsed[32] dd, $J = 431$, 16, $J_{Pt-P} = 2796$), 56.0 (dd, $J = 16$, 9, $J_{Pt-P} = 3918$); diastereomer **b**, δ 65.7 (dd, $J = 432$, 9), 60.8 (dd, $J = 432$, 17), 60.1 (dd, $J = 16$, 9, $J_{Pt-P} = 3913$). ^1H NMR (CD_2Cl_2): δ 7.70−7.65 (m, 1H, Ar), 7.62−7.54 (m, 3H, Ar), 7.05 (2H, Ar), 4.80−4.68 (m, 2H), 3.20−3.08 (m, 1H), 3.08−2.90 (m, 2H), 2.90−2.80 (m, 1H), 2.55−2.30 (m, 4H), 2.15−2.03 (m, 2H), 2.03−1.90 (m, 4H), 1.75−1.61 (m, 2H), 1.503 (dd, $J = 20$, 7, 3H, Me), 1.495 (dd, $J = 18$, 7, 3H, Me), 1.23 (d, $J = 7$, 6H, Me), 1.204 (d, $J = 7$, 6H, Me), 1.20 (d, $J = 7$, 6H, Me), 0.86 (dd, $J = 16$, 8, 3H, Me), 0.73 (dd, $J = 16$, 8, 3H, Me). $^{13}C\{^1H\}$ NMR (CD_2Cl_2): δ 152.8 (quat), 149.6 (quat), 139.3 (d, $J = 24$, quat), 138.2 (d, $J = 27$, quat), 133.3−133.0 (m, quat), 132.55 (Ar), 132.45 (Ar), 132.0 (d, $J = 6$, Ar), 131.4 (d, $J = 3$, Ar), 121.9 (apparent t, $J = 4$), 46.0 (d, $J = 39$), 41.9 (d, $J = 16$), 41.7 (d, $J = 14$), 38.0, 37.5, 37.0, 36.7 (d, $J = 14$), 36.5 (d, $J = 15$), 34.7 (d, $J = 6$), 34.4, 30.3, 26.7 (2Me, Is), 25.1 (2Me, Is), 24.0 (2Me, Is), 16.60 (d, $J = 5$), 16.56 (d, $J = 4$), 16.3 (d, $J = 4$), 14.6, 13.7 (d, $J = 2$).

Pt((*R*,*R*)-Me-Duphos)(P(O)MeIs)$_2$ (12). To a yellow solution of bis(phosphido) complex **5** containing ~20% of chloro complex **4** and Pt((*R*,*R*)-Me-Duphos)$(OSiMe_3)$(PMeIs) as impurities (49 mg, 0.049 mmol) in 0.5 mL of toluene in an NMR tube fitted with a rubber septum was added H_2O_2 (30% in H_2O, 28 μL, 0.25 mmol), with a microliter syringe. The reaction mixture became colorless, and gas evolved. ^{31}P NMR spectroscopy indicated disappearance of the starting material. The solvent was removed under vacuum, and the white residue was washed with ether (3 × 0.5 mL). Drying the precipitate yielded 45 mg (89%) of white powder. Recrystallization from CD_2Cl_2/ether at 5 °C gave 35 mg (69%) of white crystals consisting of a 1:1 mixture of diastereomers **a** and **b**.

HRMS (*m*/*z*): calcd for $C_{50}H_{81}O_2P_4Pt^+$ (MH^+), 1031.4814; found, 1031.4810. Anal. Calcd for $C_{50}H_{80}O_2P_4Pt$: C, 58.18; H, 7.81. Calcd for $C_{50}H_{80}P_4PtO_2{\cdot}0.3CD_2Cl_2$ (recrystallization solvent): C, 57.12; H, 7.68. Found: C, 57.21; H, 6.98. $^{31}P\{^1H\}$ NMR (CD_2Cl_2): δ 60.6 (dm, $J = 365$, $J_{Pt-P} = 1656$), 51.3 (dm, $J = 360$, $J_{Pt-P} = 1864$), 50.4 (dm, $J = 362$, $J_{Pt-P} = 2954$), 48.1 (dm, $J =$

(32) The ^{31}P NMR signals for the phosphido oxide and one of the Duphos P atoms were accidentally coincident in this diastereomer, resulting in a single overlapping signal. The expected large J_{PP}[22] was observed in the Pt satellites. For similar observations in Pt−phosphine complexes, see: (a) Sperline, R. P.; Beaulieu, W. B.; Roundhill, D. M. *Inorg. Chem.* **1978**, *17*, 2032−2035. (b) Brown, M. P.; Fisher, J. R.; Puddephatt, R. J.; Seddon, K. R. *Inorg. Chem.* **1979**, *18*, 2808−2813. (c) Gukathasan, R. R.; Morris, R. H.; Walker, A. *Can. J. Chem.* **1983**, *61*, 2490−2492.

359, $J_{Pt-P} = 3185$). ^1H NMR (CD_2Cl_2): δ 7.78−7.73 (m, 1H, Ar), 7.64−7.57 (m, 1H, Ar), 7.56−7.48 (m, 2H, Ar), 7.09 (1H, Ar), 7.08 (1H, Ar), 7.04 (1H, Ar), 6.95 (1H, Ar), 5.64−5.53 (m, 1H), 5.38−5.27 (m, 1H), 4.56−4.47 (m, 1H), 4.12−4.05 (m, 1H), 3.32−3.20 (m, 1H), 3.08−2.97 (m, 1H), 2.90−2.78 (m, 2H), 2.65−2.51 (m, 1H), 2.48−2.30 (m, 3H), 2.30−2.22 (m, 2H), 2.22−2.14 (m, 3H), 2.01−1.88 (m, 3H, Me), 1.79 (dd, $J = 18$, 7, 3H, Me), 1.71−1.62 (overlapping m, 4H, Me + 1H), 1.58 (dd, $J = 18$, 7, 3H, Me), 1.45 (d, $J = 6$, 3H, Me), 1.28−1.25 (overlapping m, 9H, Me), 1.23−1.18 (overlapping m, 12H, Me), 1.145 (d, $J = 7$, 3H, Me), 1.141 (d, $J = 7$, 3H, Me), 1.07 (d, $J = 7$, 3H, Me), 1.02 (d, $J = 7$, 3H, Me), 0.72 (dd, $J = 16$, 7, 3H, Me), 0.37 (dd, $J = 15$, 7, 3H, Me).

Reaction of 1 with [Pd(allyl)Cl]$_2$. Formation of PMe(Is)(allyl) (13). To a yellow solution of phosphido complex **1** (49.7 mg, 0.06 mmol) in 0.3 mL of toluene was added [Pd(allyl)Cl]$_2$ (11 mg, 0.03 mmol) in 0.2 mL of toluene. The reaction mixture turned brown immediately. It was transferred to an NMR tube and monitored by ^{31}P NMR spectroscopy. Pt((*R*,*R*)-Me-Duphos)(Ph)(Cl) (δ 67.6 ($J_{Pt-P} = 1618$), 55.7 ($J_{Pt-P} = 3892$)) was the major (>90%) Pt-Duphos-containing species. Some unidentified materials (δ 58.8, 57.7, −37.5, −51.7), PMeIs(allyl) (δ −48.6), and multiplets assigned to Pd−PMeIs(allyl) species (δ 25.6−24.8, −9.1 to −9.5, −10.0 to −10.4, −13.2 to −13.6, −13.9 to −14.4, −15.9 to −16.4, −16.8 to −17.2) were observed.

A solution of dppe (48 mg, 0.12 mmol) in 0.1 mL of toluene was added to the reaction mixture. Pt(Me-Duphos)(Ph)(Cl), Pd(dppe)$_2$ (δ 32.0), dppe (δ −11.6), and PMeIs(allyl) (δ −49.1) were observed in the mixture. The solvent was removed under vacuum, and a 9:1 petroleum ether−THF mixture (0.5 mL) was added to the residue. Pt((*R*,*R*)-Me-Duphos)(Ph)(Cl) was removed from the reaction mixture on a silica column (5 cm height, 0.6 cm diameter), using a 9:1 petroleum ether−THF mixture as eluent; the Pt complex did not elute. The solvent was removed under vacuum, and 39 mg of an off-yellow powder was obtained. The mixture consisted of Pd(dppe)$_2$, dppe, and PMeIs(allyl). Chromatography on a silica column (5 cm height, 0.6 cm diameter), using petroleum ether eluent, gave a solution of the allylphosphine (Pd(dppe)$_2$ and dppe did not elute). The solvent was removed under vacuum, and 12 mg (71% yield) of a colorless oil was obtained. The tertiary phosphine was dissolved in 0.5 mL of C_6D_6 for spectroscopic characterization, which showed it was 94% pure (by ^{31}P NMR).

Both the protonated phosphine and the protonated phosphine oxide were observed by mass spectroscopy. HRMS (*m*/*z*): calcd for $C_{19}H_{32}P^+$(MH^+), 291.2242; found, 291.2237. HRMS (*m*/*z*): calcd for $C_{19}H_{32}OP^+$ (MOH^+), 307.2191; found, 307.2196. $^{31}P\{^1H\}$ NMR (C_6D_6): δ −49.1 (purity 94%, other peak −38.2). ^1H NMR (C_6D_6): δ 7.13 (d, $J_{P-H} = 3$, 2H, Ar), 5.94−5.83 (m, 1H, CH allyl), 5.05−4.99 (ddm, $J_{P-H} = 5$, $J = 18$, 1, 1H, allyl), 4.94−4.91 (dm, $J = 10$, 1H, allyl), 4.18−4.08 (m, 2H, *i*-Pr), 2.79−2.67 (overlapping m, 3H, P−CH_2 + CH, i-Pr), 1.42 (d, $J_{P-H} = 6$, 3H, P−Me), 1.31 (d, $J = 7$, 6H, CH_3), 1.30 (d, $J = 7$, 6H, CH_3), 1.20 (d, $J = 7$, 6H, CH_3). $^{13}C\{^1H\}$ NMR (C_6D_6): δ 156.3 (d, $J = 21$, quat), 150.9 (quat), 135.9 (d, $J = 23$, CH allyl), 130.8 (d, $J = 41$, quat), 122.6 (d, $J = 6$, Ar), 116.3 (d, $J = 19$, CH_2 allyl), 35.4 (d, $J = 25$, P−CH_2), 35.0 (CH, *i*-Pr), 31.8 (d, $J = 34$, CH, *i*-Pr), 25.5 (d, $J = 1$, CH_3), 25.4 (CH_3), 24.4 (d, $J = 2$, CH_3), 11.7 (d, $J = 32$, P−CH_3).

Determination of ee. The tertiary phosphine (8 mg, 0.027 mmol) was dissolved in 0.5 mL of C_6D_6. This solution was added to (*S*)-{Pd[$NMe_2CH(Me)C_6H_4$](μ-Cl)}$_2$ (8 mg, 0.014 mmol), and the mixture was transferred to an NMR tube. The ee was determined by integration of the ^{31}P NMR signals of the diastereomers. $^{31}P\{^1H\}$ NMR (C_6D_6): δ 9.6, 9.1; ratio 1:3, 51% ee.

Reaction of 1 with Pd(P(*o*-Tol)$_3$)$_2$. Generation of Pt((*R*,*R*)-Me-Duphos)(Ph)(μ-PMe(Is))(Pd(P(*o*-Tol)$_3$)) (14). Complex **1** (83 mg, 0.1 mmol) in toluene (1 mL) was added to a slurry of Pd(P(*o*-Tol)$_3$)$_2$ (72 mg, 0.1 mmol) in toluene (1 mL). The mixture turned brown immediately, but unreacted Pd(P(*o*-Tol)$_3$)$_2$ was still observed as a light-colored precipitate. A sample of the reaction mixture was transferred into an NMR tube and monitored by ^{31}P NMR spectroscopy. After 10 min, complex **14** (as a 1:1 mixture of two diastereomers **a** and **b**) and P(*o*-Tol)$_3$ were the major components of the mixture, along with unreacted **1**. After 20 h, a light-colored precipitate was still present, but Pd(P(*o*-Tol)$_3$)$_2$ was observed in solution by ^{31}P NMR spectroscopy. The ratio **14**:P(*o*-Tol)$_3$:**1**:Pd(P(*o*-Tol)$_3$)$_2$ was 22.2:14.0:2.6:1; standing for 4 days caused small changes in the ratio, but the reaction did not proceed to completion.

The LRMS spectrum of this mixture showed peaks corresponding to PdP(*o*-Tol)$_3$ (*m*/*z* 411), Pd(P(*o*-Tol)$_3$)$_2$ (*m*/*z* 715.3), Pt(Me-Duphos)(Ph) (*m*/*z* 579.4), and Pt(Me-Duphos)(Ph)(P(O)(Me)(Is)) (*m*/*z* 844.4). The following NMR spectra are reported for the mixture of two diastereomers.

Pt((*R*,*R*)-Me-Duphos)(Ph)(μ-PMe(Is))(Pd(P(*o*-Tol)$_3$)) (14). $^{31}P\{^1H\}$ NMR (toluene): δ 57.0 (dd, $J = 244$, 7, $J_{Pt-P} = 1839$), 55.564 (dd, $J = 248$, 7, $J_{Pt-P} = 1845$), 55.560 ($J_{Pt-P} = 1864$), 52.6 ($J_{Pt-P} = 1819$), 0.2 (d, $J = 234$), −0.7 (d, $J = 230$), −35.0 (overlapping dd, $J \approx 248$, 234, $J_{Pt-P} = 1592$), −42.6 (overlapping dd, $J \approx 244$, 230, $J_{Pt-P} = 1507$).

Pd(P(*o*-Tol)$_3$)$_2$. $^{31}P\{^1H\}$ NMR (toluene): δ −6.4.

P(*o*-Tol)$_3$. $^{31}P\{^1H\}$ NMR (toluene): δ −28.5.

X-ray Crystallography. Crystallographic data are collected in Table 3. All diffraction data were collected on Bruker diffractometers equipped with APEX CCD detectors at the temperatures shown. All data were corrected for absorption using empirical (multiscan) methods. Space group assignments were unambiguous for chiral molecules. All structures were refined using anisotropic thermal parameters for non-hydrogen atoms, and hydrogen atoms were treated as idealized contributions. Absolute stereochemistries were determined by the values of the Flack parameters. For **9**, a molecule of highly disordered methylene chloride was rendered using SQUEEZE, which treats electron densities in void spaces as diffuse contributions. All software used was contained in either the libraries distributed by Bruker AXS (Madison, WI) or in the PLATON suite of programs by A. Spek.

Acknowledgment. We thank the National Science Foundation for support.

Supporting Information Available: Details of the X-ray structure determinations (CIF files and tables). This information is available free of charge via the Internet at http://pubs.acs.org.

OM060614Y